

New Construction of Black Hole Solution in Non-Commutative Geometry and their Thermodynamic Properties

Abdellah Touati ^{1,*}

¹*Department of Physics, Faculty of Exact Sciences, University of Bouira, Algeria.*

We present a new method to construct black hole solutions in non-commutative (NC) gauge theory. First we obtain the NC correction to the Newton potential via the Seiberg-Witten (SW) map, and then solve the Einstein equations in the presence of the resulting NC matter density at first order in the NC parameter. The same procedure is applied to construct a charged solution with NC $U(1)$ symmetry. This method yields an exact black hole solution in NC gauge theory at the stated order and is considerably less cumbersome than other NC gauge theory approaches to gravity. As an application, we analyze the thermodynamic properties of the new solutions: we compute the ADM mass, Hawking temperature, entropy, heat capacity and free energy, both in the absence and in the presence of pressure. Our results show that non-commutativity removes the temperature divergence at the final stage of evaporation and induces a second-order phase transition; in the presence of pressure we recover a Hawking-Page-like phase transition. We then investigate the susceptibility and linear response of the black hole to changes in the NC parameter. Our results show high sensitivity to small changes in the NC parameter for small black holes, while the sensitivity becomes weaker for larger ones. Finally, we study quantum tunneling in this geometry for both thermal and non-thermal radiation, and we investigate the particle-number density and statistical correlations of successive emissions. We find that the NC deformation suppresses the particle-number density and weakens correlations between successive emissions, effectively acting as a barrier to particle escape.

Keywords: Non-commutative gauge theory, Black hole thermodynamic, Quantum tunneling, Particle number density, Statistical correlation

CONTENTS

I. Introduction	2
II. Construction of the non-commutative black hole via gauge theory	3
A. Non-commutative Schwarzschild black hole	4
1. Geometrical properties	5
B. Non-commutative charged black hole	6
1. Geometrical properties	8
III. Thermodynamic properties	8
A. ADM mass, Hawking temperature, Entropy	9
1. Hawking temperature	9
2. Entropy	10
3. Heat capacity and phase transition	11
B. Gibbs free energy	12
C. Non-commutative susceptibility and Linear Response	13
D. Thermodynamic properties of the NC charged black hole	14
IV. Quantum tunneling process	15
A. Pure thermal radiation	16
1. Tunneling rate in thermal radiation	16
2. Density number of particles	17
B. Non-thermal radiation	17
1. Correlations	18
V. Conclusion	19

* touati.abph@gmail.com

A. Non-commutative correction to the Schwarzschild-De-Sitter black hole	20
B. Non-commutative correction to the Reissner-Nordström-De-Sitter black hole	21
Acknowledgments	22
References	22

I. INTRODUCTION

Recently there has been considerable interest in unification theories that attempt to unify gravity, as described by general relativity, with the electromagnetic, weak and strong interactions described by the Standard Model. These two frameworks are among the most successful theories in modern physics: general relativity describes gravitational interaction at the macroscopic scale, while the Standard Model describes the fundamental interactions at the quantum scale. However, when one attempts to apply the gravitational interaction to quantum systems, its effect is negligible compared to other interactions that dominate at this scale; this is due to the relative weakness of Newton's constant compared to the coupling strengths of the strong, weak and electromagnetic interactions, and it is one reason why unification is difficult. In this context, several theories and models have emerged that aim to describe gravity at the quantum scale and thereby make its effects significant enough to allow unification with the other interactions. Among the most promising approaches that provide theoretical backgrounds for quantum gravity are string theory (ST), which predicts the graviton as the mediator of the gravitational force [1–3]; loop quantum gravity (LQG), which presents a nonperturbative framework based on the quantization of geometry (area and volume) [4, 5] and can be applied to black hole physics [6, 7]; and supergravity (SG) [8–11]. We also mention the semi-classical approach pioneered by Hawking [12]. Unfortunately, none of these approaches has been confirmed experimentally, despite their impressive applications and theoretical results.

The first bridge toward a quantum-gravity picture that combined aspects of quantum field theory and gravity in a semi-classical setting was proposed by S. Hawking in 1975 [12]. By applying quantum field theory near the event horizon, Hawking discovered black hole radiation and evaporation [12, 13], analogous to black-body radiation. This phenomenon of radiation and evaporation enabled the application of thermodynamic laws to black holes [14], treating these objects as thermodynamical systems. Hawking's results opened the way to the large research area of black hole phenomenology [13, 15–26]. Subsequently, several other approaches were developed to derive black hole radiation in parallel with the original model [12]. These include anomaly mechanisms methods near the horizon [27–29], which reproduce Hawking radiation, and quantum tunneling methods in a semi-classical framework [30–33], which describe particle tunneling across the horizon. These techniques have proved invaluable for studying radiation from a variety of static, spherically symmetric black holes [34–41].

Despite the successes of Hawking's semi-classical approach [12] in predicting black hole evaporation, it faces problems at the final stage of evaporation and does not resolve the singularities inside black holes. The semi-classical treatment is applicable only in the exterior near-horizon region; in the deep interior, thermodynamic laws break down and a full quantum-gravity description becomes necessary. In this context many phenomenological models have been proposed to capture quantum-gravity effects (alongside the theories mentioned above, such as ST, LQG and SG). Examples include rainbow gravity [42, 43], generalized uncertainty principle (GUP) and extended uncertainty principle (EUP) frameworks [44–52], and NC geometry [53]. These models typically predict a minimal length that acts as a natural cutoff removing singular behavior and is expected to be of the order of the Planck scale, where gravitational effects become significant.

In this context NC geometry is one of the most promising approaches to describe quantum gravity effects. The main idea is to quantize spacetime itself, thereby introducing quantum-gravity effects through the non-commutativity of coordinates. Such quantum-gravity effects are expected to be relevant in strong gravitational fields and negligible in the low-energy limit. This approach is motivated in part by string theory [54, 55], which provides tools to regularize Hawking divergences via spacetime quantization. Recently, there has been much interest in the study of thermodynamic properties, thermal stability, and phase transitions of black holes in this geometry using different implementations. These include deformed mass models using smeared energy distributions with various profiles, e.g., Lorentzian distributions [56, 57] and Gaussian distributions [58, 59], geometric corrections via Bopp's shift [60, 61], formulations based on NC gauge theory of gravity built from the SW map [54] and the star product [62–65]¹. Here we aim to study thermodynamic properties of black holes in the presence of NC geometry using the NC gauge-theory formulation based on the SW map.

Our work is situated in the same context: motivated by the quantum-scale origin of spacetime non-commutativity and by earlier deformed-mass constructions based on smeared mass and charge distributions [58, 68], we introduce a new

¹ These papers was made it using the model developed by A. H. Chamseddine [66], which is based on missing term that was reported recently in Ref. [67].

construction of black hole solutions within NC gauge theory. In our approach, spacetime non-commutativity is imposed at the level of the interaction potentials prior to solving the Einstein equations. Using a SW-map-inspired deformation of the Newton and Coulomb potentials [54], the deformed potentials encode both the NC structure and the interaction dynamics. This perspective complements the widely used smeared mass/charge prescriptions (where NC effects enter through modified matter or charge distributions) by allowing NC physics to modify the source terms directly through the interaction. Since this geometry is expected to emerge at high (quantum) energies, introducing it via the quantum interaction potential is a natural way to capture quantum-scale corrections to the source terms. We derive the effective energy-momentum tensor generated by the deformed interaction potential, solve the Einstein equations, and analyze the resulting NC black hole solutions. In particular, we compute the ADM mass, temperature, and entropy, and study thermal stability and phase structure via heat capacity and free energy, where we examine the role of pressure on phase transitions, and study the susceptibility of the geometry to changes in the deformation parameter. Finally, we evaluate the impact of this geometry on the quantum tunneling process for both thermal and non-thermal scenarios, as well as on particle number densities and statistical correlations between successive emissions.

This paper is organized as follows. In Sec. II, we present a new model to construct an NC black hole based on NC gauge theory by solving the Einstein equations in the presence of an NC Newton potential at first order in the NC parameter, and we generalize the construction to the $U(1)$ potential for charged black holes. In Sec. III, we study thermodynamic properties of the new black hole solution, where we examine the impact of this geometry on the ADM mass, temperature, and entropy as functions of the NC parameter. We then investigate phase transitions and thermal properties by analyzing the profiles of the heat capacity and both Helmholtz and Gibbs free energies in the presence of this geometry. We also investigate the NC susceptibility function of this black hole to describe its sensitivity to changes in the deformation parameter. In Sec. IV, we study black hole radiation as a quantum-tunneling process of massless particles from the NC black hole in the context of NC gauge theory, considering two scenarios: thermal and non-thermal radiation. We also investigate particle number densities and correlations between successive emissions in this approach. Finally, Sec. V, contains our concluding remarks.

II. CONSTRUCTION OF THE NON-COMMUTATIVE BLACK HOLE VIA GAUGE THEORY

In this section we briefly review NC geometry and NC gauge theory via the SW map, and we present a new construction of black hole solutions for studying the effects of this geometry by imposing NC structure on the interaction potential prior to solving the Einstein equations via the SW map [54]. In this case the Einstein equations read

$$G_{\mu\nu} = R_{\mu\nu} - \frac{1}{2}g_{\mu\nu}R = \frac{8\pi G}{c^2} \hat{T}_{\mu\nu}, \quad (1)$$

where $\hat{T}_{\mu\nu}$ is the energy-momentum tensor that encodes both quantum-geometry effects and the interaction dynamics.

In this work we consider static, spherically symmetric black hole solutions with a Schwarzschild-like metric,

$$ds^2 = -f(r) c^2 dt^2 + \frac{dr^2}{f(r)} + r^2 d\theta^2 + r^2 \sin^2 \theta d\phi^2, \quad (2)$$

which we use below to solve the Einstein equations in the presence of the deformed potential and thereby determine the lapse (curvature) function $f(r)$ for each case.

The basic idea of our approach is that one may probe quantum-gravity effects by quantizing spacetime itself; NC geometry provides a convenient effective framework for this purpose. The geometry of NC spacetime is characterized by the following commutation relation between the coordinate operators [53]:

$$[\hat{x}^\mu, \hat{x}^\nu] = i\Theta^{\mu\nu}, \quad (3)$$

where $\Theta^{\mu\nu}$ is a real, antisymmetric matrix. In this theory the ordinary product of two functions $f(x)$ and $g(x)$ is replaced by the \star -product (Moyal product); explicitly,

$$f(x) \star g(x) = \exp\left(\frac{i}{2} \Theta^{\mu\nu} \partial_\mu \partial'_\nu\right) f(x) g(x') \Big|_{x'=x}. \quad (4)$$

The NC gauge theory was developed by N. Seiberg and E. Witten [54], where they found an important gauge transformation that gives a correspondence between the ordinary gauge fields and the NC gauge ones. This transformation is called the SW map and is given by

$$\hat{A}(A, \Theta) + \delta_\lambda \hat{A}(A, \Theta) = \hat{A}(A + \delta_\lambda A, \Theta), \quad (5)$$

where δ_λ and $\delta_{\hat{\lambda}}$ denote the infinitesimal variations under the commutative and NC gauge transformations, respectively. By using this map, we express the deformed gauge potential \hat{A} as a power series in Θ up to first order [54]:

$$\hat{A}_\mu = A_\mu - \frac{g}{2} \Theta^{\alpha\beta} A_\alpha (\partial_\beta A_\mu + F_{\beta\mu}) + \mathcal{O}(\Theta^2), \quad (6)$$

where g is the coupling constant of the interaction. Moreover, this geometry leads to the emergence of self-interactions of the gauge field, with the NC parameter acting as an effective coupling constant. Such interactions are not present in the commutative $U(1)$ gauge potential. This can therefore be interpreted as a new type of quantum interaction generated by the NC structure of spacetime itself.

The NC matrix for general form is given by:

$$\Theta^{\mu\nu} = \begin{pmatrix} 0 & a_1 & a_2 & a_3 \\ -a_1 & 0 & d_1 & d_2 \\ -a_2 & -d_1 & 0 & d_3 \\ -a_3 & -d_2 & -d_3 & 0 \end{pmatrix}, \quad \mu, \nu = 0, 1, 2, 3. \quad (7)$$

In this work we have use only the first component of gauge potential A_t with static and radial in spherical symmetric, for that the only non-zero NC correction is come from $a_1 = \Theta$, and for the rest we can set them zero.

A. Non-commutative Schwarzschild black hole

In order to obtain the NC correction to a black hole we start by correcting the Newton potential for gravity via the SW map. To apply this map to the gravitational potential we use the gravito-electromagnetic potential notation $\mathcal{A}_\mu(r) = (\Phi_N(r)/c, 0, 0, 0)$, with the scalar potential $\Phi_N(r)$ given by the Newton potential:

$$\Phi_N(r) = -\frac{GM}{r} \quad (8)$$

To describe the NC correction to this potential, we employ an NC gauge theory via the SW map, which yields

$$\hat{\Phi}_N(r) = -\frac{GM}{r} + \frac{\Theta}{l_p c^2} \frac{G^2 M^2}{r^3} \quad (9)$$

where the coupling charge in the case of gravity is taken to be $g = m_p/(\hbar c)$.² From now on we set $\tilde{\Theta} = \Theta/l_p$ as a new NC parameter with dimensions of length.

Next we obtain the contribution of NC geometry to the Newtonian mass density. The Poisson relation $\nabla^2 \hat{\Phi}_N(r) = 4\pi G \hat{\rho}$ for the exterior region $r > 0$ yields

$$\hat{\rho} = 3 \frac{\tilde{\Theta} G M^2}{2\pi c^2 r^5}. \quad (10)$$

For a spherically symmetric matter distribution the energy-momentum tensor can be written in the perfect-fluid diagonal form [69]:

$$[\hat{T}^\mu{}_\nu] = \text{diag}(-\hat{\rho}, \hat{p}_r, \hat{p}_\theta, \hat{p}_\phi). \quad (11)$$

To preserve the Schwarzschild-like form of the metric the radial pressure must satisfy $p_r = -\rho$, which together with the conservation equations implies a tangential pressure $\hat{p}_\theta = -\hat{\rho} - \frac{r}{2} \partial_r \hat{\rho}$. The temporal and radial components of the energy-momentum tensor in our case read

$$\hat{T}_0^0 = \hat{T}_r^r = -\frac{3GM^2}{2\pi r^5} \tilde{\Theta}. \quad (12)$$

For a Schwarzschild-like metric the lapse (curvature) function has the form

$$f(r) = 1 - \frac{2Gm(r)}{c^2 r}, \quad (13)$$

² We have used the standard Planck-unit definitions $l_p = \sqrt{\hbar c^3/G}$ and $m_p = \sqrt{\hbar c/G}$. After simple algebra one obtains $m_p/(\hbar c) = 1/(l_p c^2)$.

where $m(r)$ is a function of r . Using metric (2) and (13), the non-vanishing components of the Einstein tensor are

$$G_0^0 = G_r^r = -\frac{2Gm'(r)}{c^2 r^2}, \quad G_\theta^\theta = G_\phi^\phi = -\frac{Gm''(r)}{c^2 r^2}. \quad (14)$$

Using the Einstein equations we obtain

$$\begin{aligned} m(r) &= M - \frac{1}{c^2} \int 4\pi r'^2 \hat{T}_0^0 dr', \\ &= M - \frac{3GM^2}{c^2 r^2} \tilde{\Theta} = M \left(1 - \frac{3m}{r^2} \tilde{\Theta} \right) \end{aligned} \quad (15)$$

where $m = \frac{GM}{c^2}$ is the Schwarzschild mass of the black hole. Note that this expression is written to first order in the NC parameter; to higher order one obtains a different compact form³. In a regularized form (in similar form to regular-like black hole, and its reduced to (15) in $\mathcal{O}(\tilde{\Theta})$) one may write

$$m(r) = \frac{Mr^2}{(r^2 + 3m\tilde{\Theta})}. \quad (16)$$

Substituting this result into (13) gives the NC Schwarzschild metric

$$f(r) = 1 - \frac{2mr}{(r^2 + 3m\tilde{\Theta})}, \quad (17a)$$

$$\simeq 1 - \frac{2m}{r} + \frac{6m^2}{r^3} \tilde{\Theta}. \quad (17b)$$

The second line is the first-order expansion, equivalent to the solution obtained in Eq. (15), while the first line has a form analogous to regular (regular-like) black-hole solutions. In our construction this solution is obtained from the gauge-theory approach to non-commutativity via the SW map correction; the compact form above is valid only to first order in the SW map parameter. In the limit $\tilde{\Theta} \rightarrow 0$ the commutative Schwarzschild metric is recovered.

1. Geometrical properties

In the following we present some geometric properties of the new black-hole solution in NC spacetime. We first consider the event horizons, which are obtained by solving $f(r_h) = 0$. The solutions are

$$r_{\pm} = m \pm \sqrt{m^2 - 3m\tilde{\Theta}} \quad (18)$$

Thus the black hole possesses two event horizons, an inner and an outer horizon. In the commutative limit $\tilde{\Theta} \rightarrow 0$ the two horizons merge and one recovers the single Schwarzschild horizon.

Fig. II A 1 shows the dependence of the outer and inner horizons r_{\pm} on the black hole mass m , together with the commutative case. The qualitative behavior resembles that of the RN metric: the NC parameter plays a role analogous to the electric charge in producing a pair of horizons. In our solution the NC event horizons are smaller than the commutative Schwarzschild radius for the chosen parameters; this trend agrees with previous NC gauge theory results [67] (although the magnitude of the effect depends on the adopted model). For other NC implementations the effect can be reversed, with the horizon increasing with non-commutativity [70]. From the right panel we clearly see that increasing $\tilde{\Theta}$ increases the inner horizon and decreases the outer horizon until they coincide; that coincidence corresponds to an extremal black hole, while larger values of $\tilde{\Theta}$ (for fixed m) lead to no black hole solution.

Fig. II A 1 displays $f(r)$ in both the first-order expansion (left panel) and the compact form (right panel) as a function of radius r/m and for different $\tilde{\Theta}$. In both representations the solution admits two event horizons given by (18). The behavior is qualitatively similar to that of the RN family (see [71, 72]): one finds three regimes determined by the sign of $m - 3\tilde{\Theta}$. If $m > 3\tilde{\Theta}$ the solution describes a black hole with two distinct horizons and a timelike curvature singularity (here $f(r) > 0$ at $r = 0$); if $m = 3\tilde{\Theta}$ the solution is extremal with a double horizon; and if $m < 3\tilde{\Theta}$ no horizon exists and the solution corresponds to a naked singularity. The same qualitative regimes are apparent in the left panel. Our SW map construction therefore yields a horizon structure similar to that obtained from point-like NC matter distributions (Lorentzian or Gaussian) and also shows similarities with certain nonlinear electromagnetic black hole models [73].

³ This expression is valid only at first order in $\tilde{\Theta}$; higher-order corrections change the compact form.

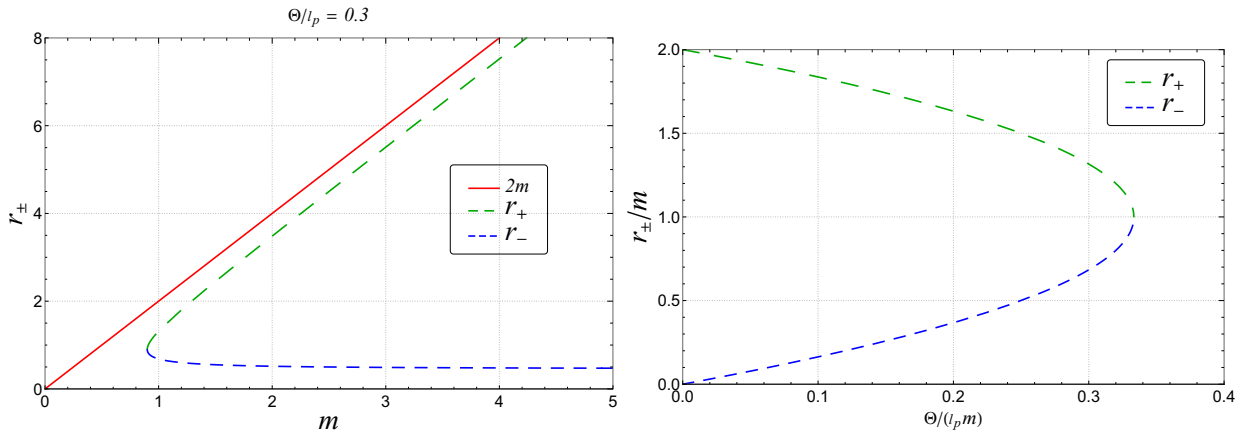


FIG. 1. Behavior of the event horizons r_{\pm} as a function of the mass for $\tilde{\Theta} = 0.3$, compared with the commutative solution $\tilde{\Theta} = 0.0$ (left panel), and as a function of the NC parameter $\tilde{\Theta}$ (right panel).

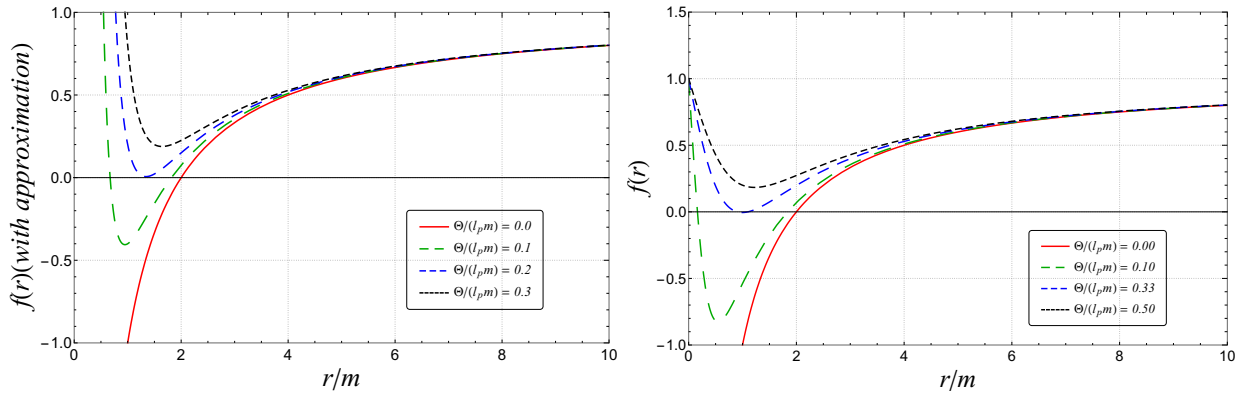


FIG. 2. Behavior of the curvature function $f(r)$ as a function of the radius r for different values of $\tilde{\Theta}$. Left panel: leading order in $\tilde{\Theta}$. Right panel: compact form.

B. Non-commutative charged black hole

In the following we consider a charged black hole whose electric potential is $A_{\mu}(r) = (\Phi_e(r)/c, 0, 0, 0)$, with the Coulomb scalar potential

$$\Phi_e(r) = \frac{q}{4\pi\epsilon_0 r}. \quad (19)$$

In analogy with the gravitational case, we apply the NC gauge theory correction to the Coulomb potential via the SW map. To first order in Θ the SW map for the gauge potential reads⁴

$$\hat{A}_{\mu} = A_{\mu} - \frac{q_p}{\hbar} \Theta^{\alpha\beta} A_{\alpha} \partial_{\beta} A_{\mu} + \mathcal{O}(\Theta^2), \quad (20)$$

where $q_p = \sqrt{4\pi\epsilon_0 \hbar c}$ is the Planck charge. After few algebra we obtain the corrected time component

$$\hat{A}_0 = \frac{q}{4\pi\epsilon_0 c r} + \frac{\Theta}{l_p} \frac{\sqrt{G} q^2}{(4\pi\epsilon_0)^{3/2} c^3 r^3}. \quad (21)$$

⁴ With coupling charge in the electromagnetic interaction take $g = q_p/\hbar$.

As before we introduce $\tilde{\Theta} = \Theta/l_p$ as the NC parameter with dimensions of length.

We now compute the energy-momentum tensor for the corrected gauge potential. In our conventions the Maxwell energy-momentum tensor (SI units) may be written as

$$(T^{\text{Maxwell}})_{\mu\nu} = \varepsilon_0 \left(F_{\mu\sigma} F_{\nu}{}^{\sigma} - \frac{1}{4} g_{\mu\nu} F_{\rho\sigma} F^{\rho\sigma} \right), \quad (22)$$

The nonzero diagonal components of the corrected Maxwell energy-momentum tensor evaluated for our \hat{A}_0 are

$$(\hat{T}^{\text{Maxwell}})_{00} = (\hat{T}^{\text{Maxwell}})_{rr} = -\frac{q^2}{32\pi^2 \varepsilon_0 r^4} - \tilde{\Theta} \frac{3\sqrt{G} q^3}{16\pi(4\pi\varepsilon_0)^{3/2} c^2 r^6}. \quad (23)$$

Substituting (23) into the Einstein equations for the Schwarzschild-like metric gives

$$\begin{aligned} m(r) &= M - \frac{1}{c^2} \int 4\pi r'^2 (\hat{T}^{\text{Maxwell}})_{00} dr' \\ &= M - \frac{q^2}{8\pi\varepsilon_0 c^2 r} - \frac{\tilde{\Theta}\sqrt{G} q^3}{(4\pi\varepsilon_0)^{3/2} c^4 r^3} \\ &= M - \frac{q^2}{8\pi\varepsilon_0 c^2 r} \left(1 + \frac{2\tilde{\Theta}Q}{r^2} \right), \end{aligned} \quad (24)$$

where we define the effective squared charge (dimension of area) as

$$Q^2 = \frac{Gq^2}{4\pi\varepsilon_0 c^4}.$$

A regular-like compact form that reproduces the first-order expression above is

$$m(r) = M - \frac{q^2 r}{8\pi\varepsilon_0 c^2 (r^2 - 2\tilde{\Theta}Q)}, \quad (25)$$

valid to first order in $\tilde{\Theta}$.

Substituting this mass function into $f(r) = 1 - 2Gm(r)/(c^2 r)$ yields the NC RN-like metric function:

$$\begin{aligned} f_Q(r) &= 1 - \frac{2m}{r} + \frac{Q^2}{(r^2 - 2\tilde{\Theta}Q)} \\ &\simeq 1 - \frac{2m}{r} + \frac{Q^2}{r^2} + \frac{2\tilde{\Theta}Q^3}{r^4}, \end{aligned} \quad (26)$$

where the second line is the first-order expansion in $\tilde{\Theta}$. In the limit $\tilde{\Theta} \rightarrow 0$ one recovers the standard RN solution.

It is worth remarking that this SW-map-based deformation yields a comparatively simple corrected metric; other approaches to introduce NC gauge theory of gravity into the metric often lead to more complicated expressions that require additional approximations [65].

One may also combine the deformed mass contribution (from the gravitational NC correction) with the deformed electromagnetic contribution by adding the corresponding energy-momentum components. Doing so gives the combined mass function

$$\begin{aligned} m(r) &= M - \frac{1}{c^2} \int 4\pi r'^2 (\hat{T}^0_0 + (\hat{T}^{\text{Maxwell}})_{00}) dr' \\ &= \frac{Mr^2}{(r^2 + 3m\tilde{\Theta})} - \frac{q^2 r}{8\pi\varepsilon_0 c^2 (r^2 - 2\tilde{\Theta}Q)} \\ &\simeq M \left(1 - \frac{3m}{r^2} \tilde{\Theta} \right) - \frac{q^2}{8\pi\varepsilon_0 c^2 r} \left(1 + \frac{2\tilde{\Theta}Q}{r^2} \right). \end{aligned} \quad (27)$$

Correspondingly, the curvature function in compact and first-order expansion forms becomes

$$\begin{aligned} f_Q(r) &= 1 - \frac{mr}{(r^2 + 3m\tilde{\Theta})} + \frac{Q^2}{(r^2 - 2\tilde{\Theta}Q)}, \\ &\simeq 1 - \frac{2m}{r} + \frac{Q^2}{r^2} + \left(\frac{6m^2}{r^3} + \frac{2Q^3}{r^4} \right) \tilde{\Theta}. \end{aligned} \quad (28)$$

1. Geometrical properties

In the following we present some geometric properties of the charged NC black hole, such as the event horizons, which are obtained from solving $f(r_+) = 0$. For the case without the deformed mass [Eq. (26)] one finds two solutions⁵ given by

$$r_{\pm} = m \pm \sqrt{m^2 - Q^2} + \left(\frac{2mQ^2 - 2m^3 \pm 2m^2 \sqrt{m^2 - Q^2} \mp Q^2 \sqrt{m^2 - Q^2}}{Q^3 - mQ^2} \right) \tilde{\Theta}. \quad (29)$$

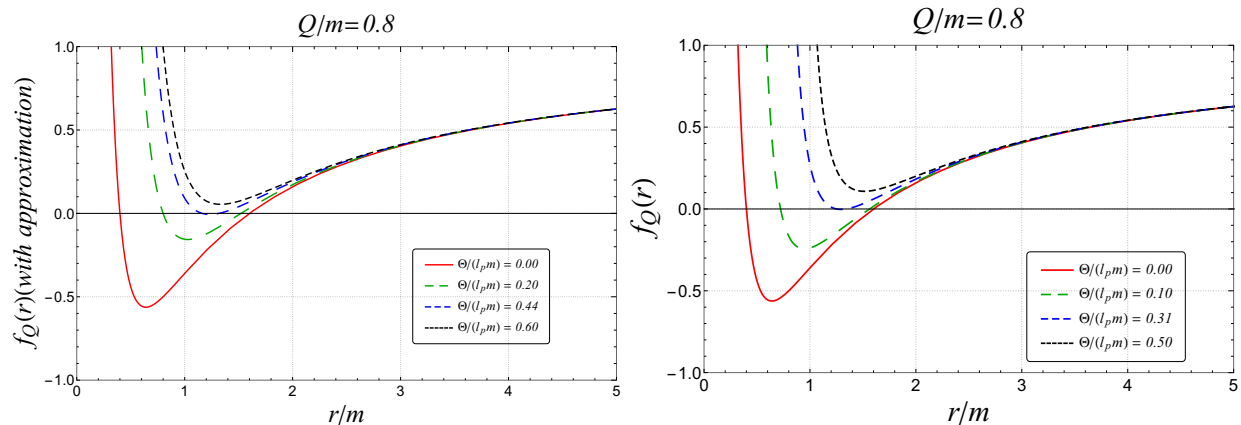


FIG. 3. Behavior of the curvature function $f(r)$ for the charged black hole (parameter Q/m) as a function of the radius r for different NC parameters $\tilde{\Theta}$. Left panel: leading order in $\tilde{\Theta}$. Right panel: compact form.

Fig. II B 1 show the variation of the curvature function $f(r)$ for the charged black hole as a function of r and for various values of the NC parameter $\tilde{\Theta}$. From the left panel we observe a qualitative similarity between the uncharged NC black hole (see left panel of Fig. II A 1) and the charged case: non-commutativity plays a role analogous to that of the electric charge, an analogy noted in several works [65, 74]. In the compact form (right panel) the profile is separated into two regions by a divergence at $r = \sqrt{2\tilde{\Theta}Q}$. For the region $r > \sqrt{2\tilde{\Theta}Q}$ the behavior mirrors the left panel: there are three regimes determined by the parameters, namely (i) a black-hole solution with two horizons for $\tilde{\Theta} < \tilde{\Theta}_c$, (ii) an extremal solution at $\tilde{\Theta} = \tilde{\Theta}_c$ with a double horizon, and (iii) no black-hole solution (naked singularity) for $\tilde{\Theta} > \tilde{\Theta}_c$ when $Q < m$. For $Q \geq m$ one typically obtains no black hole solution⁶.

III. THERMODYNAMIC PROPERTIES

In this section we investigate in detail the thermodynamic properties induced by the NC deformation via the SW map for the Schwarzschild black hole. Previous works studied NC effects by deforming the metric itself [62, 63, 75, 76]. By contrast, here we introduce non-commutativity at the level of the interaction potential prior to solving the Einstein equations (see Sec. II), which yields new NC black-hole solutions that are less complicated to analyze. In this investigation we use the standard geometric approach to black hole thermodynamics. The first law is written as

$$dm = T dS, \quad (30)$$

where m , T and S denote the ADM mass, the Hawking temperature, and the black hole entropy, respectively.

⁵ Note that both solutions formally satisfy $f(r_+) = 0$; however, the inner-horizon solution may become inconsistent with numerical and graphical results due to the leading-order approximation in the NC parameter. The perturbative expansion becomes unreliable near the extremal regime and for small radii, so the inner-horizon expression should be used with caution.

⁶ For the region $r < \sqrt{2\tilde{\Theta}Q}$ the curvature function becomes negative whatever the value of the NC parameter $\tilde{\Theta}$ and electric charge Q , which is not allowed in the approximation form.

A. ADM mass, Hawking temperature, Entropy

As a first step we compute the ADM mass of the NC Schwarzschild black hole by solving $f(r_+) = 0$ for m , where r_+ is the outer NC event horizon (see Eq. (18)). The ADM mass is

$$m = \frac{r_+^2}{2r_+ - 3\tilde{\Theta}}. \quad (31)$$

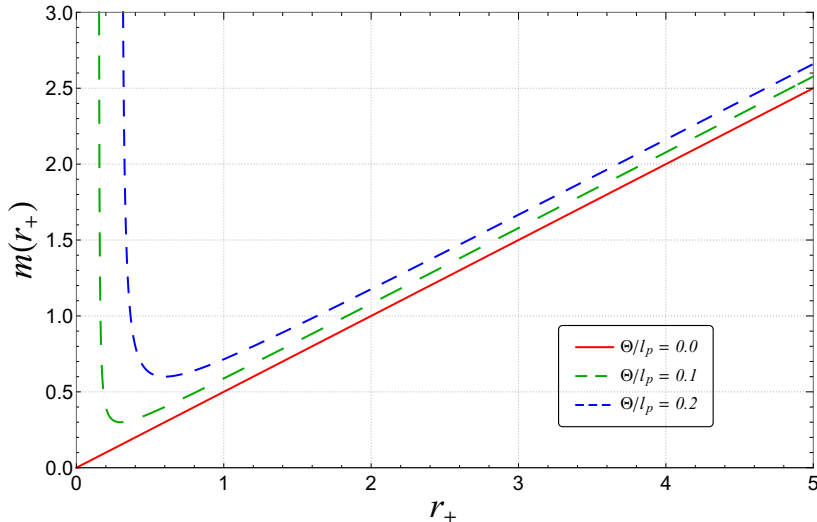


FIG. 4. Behavior of the mass parameter $m(r_+)$ as a function of the NC outer horizon r_+ for different values of the NC parameter $\tilde{\Theta}$.

Fig. III A shows the ADM mass profile $m(r_+)$ as a function of the NC horizon r_+ for several values of $\tilde{\Theta}$. (We plot only the positive branch for $r_+ > 3\tilde{\Theta}/2$.) In the commutative limit $\tilde{\Theta} = 0$ one recovers the linear relation $m = r_+/2$, which vanishes as $r_+ \rightarrow 0$. In the NC model the mass profile develops a minimum $m^{\min} = 3\tilde{\Theta}$ attained at $r_+^{\min} = 3\tilde{\Theta}$, consistent with analogous results in NC gauge theory models [62, 63, 76]. We emphasise that thermodynamic quantities should be studied as functions of the NC event horizon r_+ (the physical size of the NC black hole) rather than the commutative horizon; using the commutative radius can lead to incorrect expressions for the NC mass and thereby to misleading thermodynamic conclusions.

1. Hawking temperature

The black hole temperature is obtained from the surface gravity via $T = \kappa/(2\pi) = f'(r_+)/(4\pi)$. Evaluating the derivative at the outer horizon gives

$$\begin{aligned} T &= \frac{1}{4\pi} f'(r) \Big|_{r=r_+}, \\ &= \frac{1}{4\pi r_+} - \frac{3\tilde{\Theta}}{4\pi r_+^2}. \end{aligned} \quad (32)$$

Fig. III A 1 displays the NC Hawking temperature $T(r_+)$ versus the NC horizon r_+ for several $\tilde{\Theta}$. The NC correction removes the divergence of the commutative temperature and produces a maximal temperature T_{\max} attained at a critical radius $r_+^{\text{crit}} = 6\tilde{\Theta}$; numerically one finds $T_{\max} \simeq 0.01/\tilde{\Theta}$ for the parameter choices used in the plots. The temperature then rapidly falls to zero at the minimal horizon $r_+^{\min} = 3\tilde{\Theta}$, coinciding with the minimum mass m^{\min} shown in Fig. III A. Thus the evaporation halts and a remnant with radius r_+^{\min} and mass m^{\min} remains. These qualitative features agree with earlier NC gauge theory of gravity results [62, 63] while the present method yields simpler analytic expressions for thermodynamic quantities.

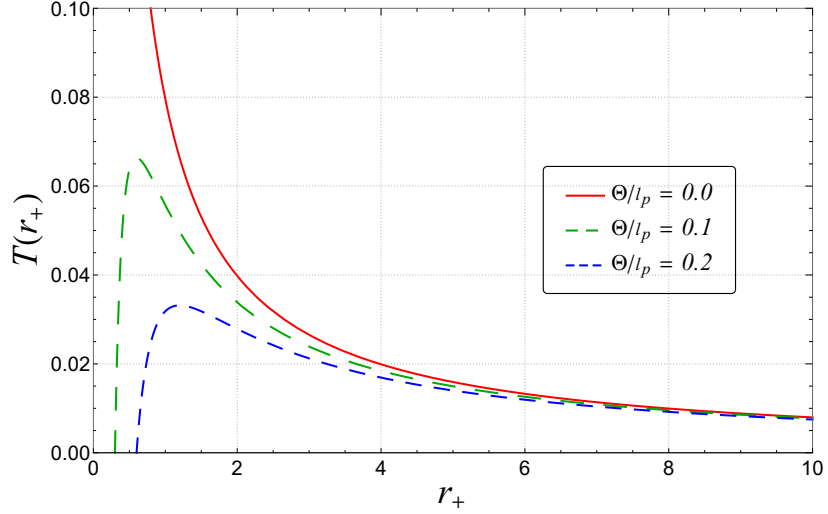


FIG. 5. Behavior of the Hawking temperature $T(r_+)$ as a function of the NC outer horizon r_+ for different values of $\tilde{\Theta}$.

We now estimate a rough bound on the NC parameter using the back-reaction scale. Taking the critical radius $r_+^{\text{crit}} = 6\tilde{\Theta}$, the characteristic thermal energy is $E \sim T_{\text{max}} \simeq 0.01/\tilde{\Theta}$, and the black hole mass at that scale (in natural units $\hbar = k_B = c = 1$) is $M = \frac{1}{2G}r_+^{\text{crit}} = 3\tilde{\Theta}M_p^2$. Equating the energy scales gives an estimate⁷ for $\tilde{\Theta} = \Theta/l_p$:

$$\tilde{\Theta} = \frac{\Theta}{l_p} \simeq 1.47 \times 10^{-35} \text{ m} \sim l_p, \quad (33)$$

and hence

$$\sqrt{\Theta} = \sqrt{\tilde{\Theta}l_p} \simeq 1.54 \times 10^{-35} \text{ m} \sim l_p. \quad (34)$$

These estimates place the NC scale close to the Planck length, consistent in order of magnitude with other NC gauge theory of gravity bounds obtained from black hole thermodynamics [62, 64, 75].

2. Entropy

We first comment on entropy in NC geometries. In many implementations of non-commutativity that including the mass source in energy-momentum tensor [77, 78], or show high order of coupling mass term from geometry correction [62, 63], in this case the NC corrections modify the area law: the entropy receives corrections and, when obtained from the first law, typically exhibits logarithmic terms at second order in the NC parameter [62].

In the present model the solid angle is not modified by non-commutativity, so the horizon area retains the commutative form,

$$A_+ = \iint \sqrt{g_{\theta\theta}g_{\phi\phi}} d\theta d\phi = 4\pi r_+^2. \quad (35)$$

In the Bekenstein-Hawking picture the entropy is proportional to the area, so at leading order one has

$$S = \frac{A_+}{4} = \pi r_+^2, \quad (36)$$

with r_+ the NC outer event horizon. In the commutative case this relation is sufficient to derive thermodynamic quantities and is consistent with the first law $T = \partial m / \partial S$. However, when NC corrections to the mass are included via the energy-momentum tensor Eq. (12), the naive area law may no longer ensure the first law in its simple form. Thus one finds

⁷ We have Take two digits after the decimal point.

generically that

$$T \neq \left(\frac{\partial m}{\partial S} \right) \quad (37)$$

unless the mass and entropy expressions are adjusted consistently. This violation of the naive area law has been observed in other NC models (NC gauge theory of gravity [62, 63], Lorentzian matter distributions [77], and Gaussian distributions [78]). Below we show that the NC RN-like solution preserves the area law and the first law in the present construction when the mass has non correction term.

The correct entropy must be obtained from the first law [75, 79],

$$S = \int \frac{dm}{T}, \quad (38)$$

and using the relations (31) and (32) one obtains

$$\begin{aligned} S &= \pi r_+^2 + 6\pi \tilde{\Theta} r_+ + \frac{27\pi}{2} \tilde{\Theta}^2 \log(2r_+ - 3\tilde{\Theta}), \\ &= \pi r_+^2 + 6\pi \tilde{\Theta} r_+ + \mathcal{O}(\tilde{\Theta}^2). \end{aligned} \quad (39)$$

At second order the entropy therefore contains a logarithmic correction, as found in other NC gauge-gravity studies [64, 75]. Because the present work focuses on first-order effects we shall use the truncated expression (last line) in what follows. Note that the logarithmic term implies the argument $2r_+ - 3\tilde{\Theta}$ must be positive; this is compatible with the restriction $r_+ > 3\tilde{\Theta}/2$ used elsewhere.

Importantly, the first-order correction implies that the entropy at the minimal horizon r_+^{\min} is nonzero, so the remnant has non-zero entropy. To force the entropy to vanish at the remnant one must include higher-order (second-order) NC corrections [64, 65, 75], which will provide further insight into the thermodynamic fate of the remnant.

3. Heat capacity and phase transition

To test thermal stability we compute the heat capacity, defined by

$$C = T \left(\frac{\partial S}{\partial T} \right) = -2\pi \frac{r_+^3}{r_+ - 6\tilde{\Theta}}, \quad (40)$$

where we used the entropy to first order (39).

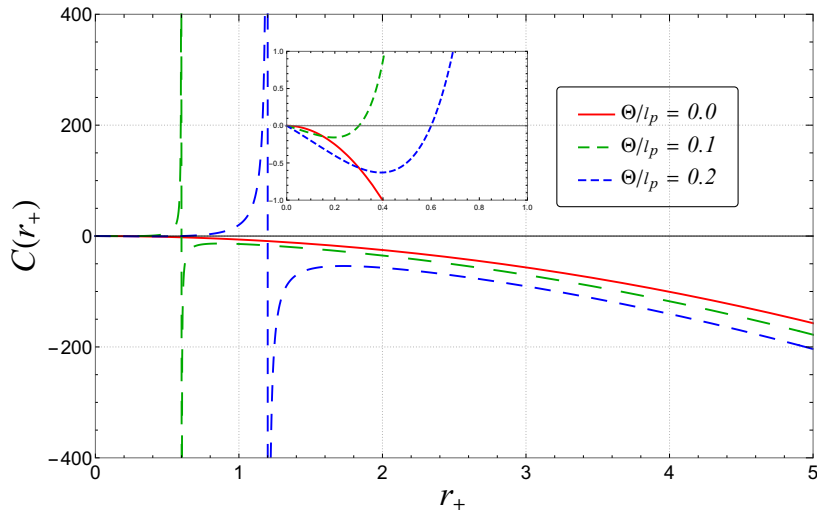


FIG. 6. Behavior of the heat capacity $C(r_+)$ as a function of the NC outer horizon r_+ for different values of $\tilde{\Theta}$.

Fig. III A 3 shows the heat capacity as a function of r_+ for several $\tilde{\Theta}$. Two characteristic points appear: (i) a divergence at $r_+ = r_+^{\text{crit}}$ and (ii) the physical limitation point $r_+ = r_+^{\text{min}}$. These points coincide with the back-reaction scale (where $T = T_{\text{max}}$) and the end of evaporation (where $T = 0$) seen in Fig. III A 1. For $r_+ > r_+^{\text{crit}}$ the heat capacity is negative and the black hole is thermodynamically unstable (non-equilibrium), while for $r_+^{\text{min}} < r_+ < r_+^{\text{crit}}$ the heat capacity is positive and the black hole is in a stable equilibrium. This behavior matches results from other NC gauge theory of gravity models [62, 63, 75]. The divergence at r_+^{crit} signals a second-order phase transition from the unstable large black hole to a stable small black hole; the critical radius increases with $\tilde{\Theta}$. The stable region $r_+^{\text{min}} < r_+ < r_+^{\text{crit}}$ also grows with $\tilde{\Theta}$, implying that larger NC parameter values prolong the final evaporation stage.

To analyze the phase structure we consider the Helmholtz free energy,

$$F = m - TS, \quad (41)$$

whose profile is shown in Fig. III A 3.

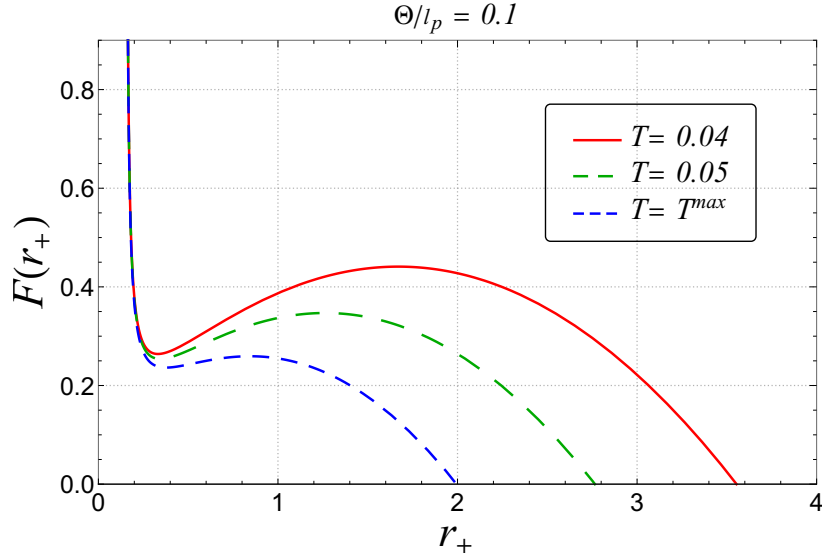


FIG. 7. Behavior of the free energy $F(r_+)$ as a function of r_+ for different temperatures T .

Fig. III A 3 shows that non-commutativity alters the free energy and generates a new minimum at the final evaporation stage [62, 63]. The free energy typically exhibits two extremals corresponding to the stable (minimum) and unstable (maximum) branches, consistent with the heat-capacity analysis.

B. Gibbs free energy

We now analyze the Gibbs free energy to study the impact of pressure on the phase structure of the NC black hole. We start from the first law of black hole thermodynamics in the presence of pressure:

$$dm = TdS - PdV, \quad (42)$$

where V denotes the NC volume of the black hole. In our geometry the volume reads

$$V = \frac{4\pi}{3}r_+^3, \quad (43)$$

and the pressure conjugate to the volume is defined by

$$\begin{aligned} \hat{P} &= - \left(\frac{\partial m}{\partial V} \right) = - \left(\frac{\partial m}{\partial r_+} \right) \left(\frac{\partial V}{\partial r_+} \right)^{-1} \\ &= - \frac{r_+ - 3\tilde{\Theta}}{2\pi r_+(2r_+ - 3\tilde{\Theta})^2} \simeq - \frac{1}{8\pi r_+^2} + \frac{9\tilde{\Theta}^2}{32\pi r_+^4}, \end{aligned} \quad (44)$$

where the leading term $P = -\frac{1}{8\pi r_+^2}$ is the commutative contribution and the NC correction appears only at second order in $\tilde{\Theta}$.

In this context we use the Gibbs free energy to characterize the influence of pressure on phase transitions for the NC Schwarzschild black hole. The Gibbs free energy is defined as

$$G = m - TS + VP. \quad (45)$$

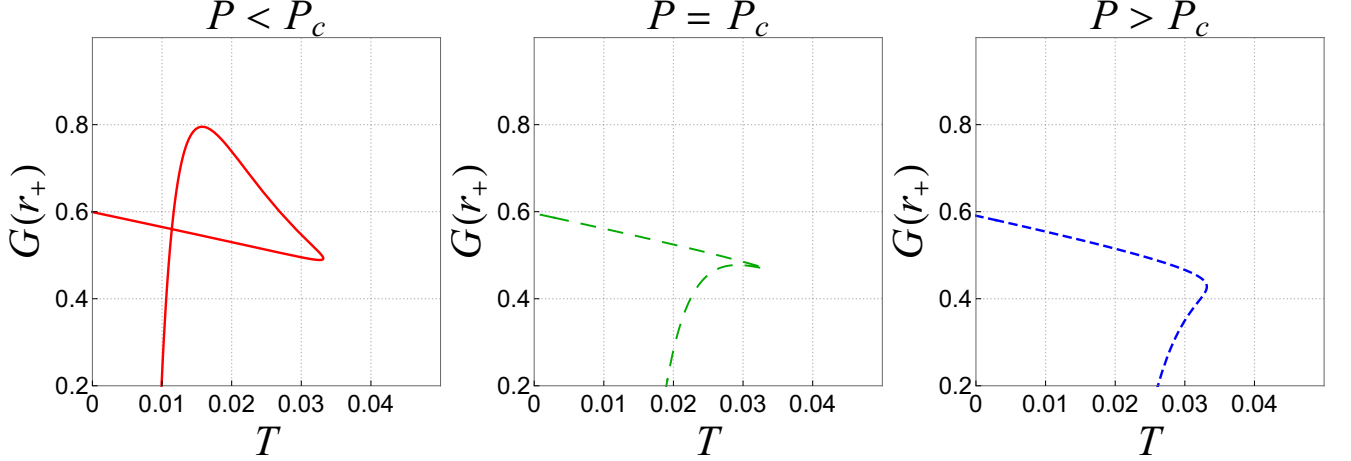


FIG. 8. Behavior of the Gibbs free energy $G(r_+)$ as a function of the temperature T for different pressures P . The plots use $\tilde{\Theta} = 0.2$ and show a critical pressure $P_c = 0.0042$.

Fig. III B displays the Gibbs free energy for $\tilde{\Theta} = 0.2$ as a function of the temperature T at several values of the pressure P . The global behavior reproduces that observed in NC gauge theory of gravity studies [62]: the present approach retains the qualitative thermodynamic features while providing a simpler framework to study NC black holes. In particular, an inflection point that signaling a Hawking-Page-like phase transition, which appears at a critical pressure $P_c \approx 0.0042$. For pressures below P_c the curve show a quasi-swallowtail structure with smooth curve; for pressures above P_c the inflection disappears and the Gibbs curve becomes smooth [62]. At the critical point the black hole undergoes a transition from a large unstable branch to a small stable branch under thermal radiation.

C. Non-commutative susceptibility and Linear Response

In this subsection we examine the linear response of the black hole to variations of the NC parameter $\tilde{\Theta}$. In this case the first law of black hole thermodynamics in the presence of NC potential reads:

$$dm = TdS + \mathcal{A}_{\tilde{\Theta}} d\tilde{\Theta}, \quad (46)$$

where $\mathcal{A}_{\tilde{\Theta}}$ represents the NC potential conjugate to the NC parameter $\tilde{\Theta}$, and is defined by [65, 80]:

$$\mathcal{A}_{\tilde{\Theta}} = \left(\frac{\partial m}{\partial \tilde{\Theta}} \right) = \frac{3r_+^2}{(2r_+ - 3\tilde{\Theta})^2}, \quad (47)$$

It is clear that this expression has the same divergence behavior as the black hole mass at the point $r_+ = \frac{3}{2}\tilde{\Theta}$; this function measures the geometric response to a change of the NC parameter.

The susceptibility of the NC parameter can be evaluated using the following definition [81, 82]:

$$\begin{aligned} \chi_{\tilde{\Theta}} &= \left(\frac{\partial \mathcal{A}_{\tilde{\Theta}}}{\partial \tilde{\Theta}} \right) = \left(\frac{\partial^2 m}{\partial \tilde{\Theta}^2} \right) \\ &= \frac{18r_+^2}{(2r_+ - 3\tilde{\Theta})^3}. \end{aligned} \quad (48)$$

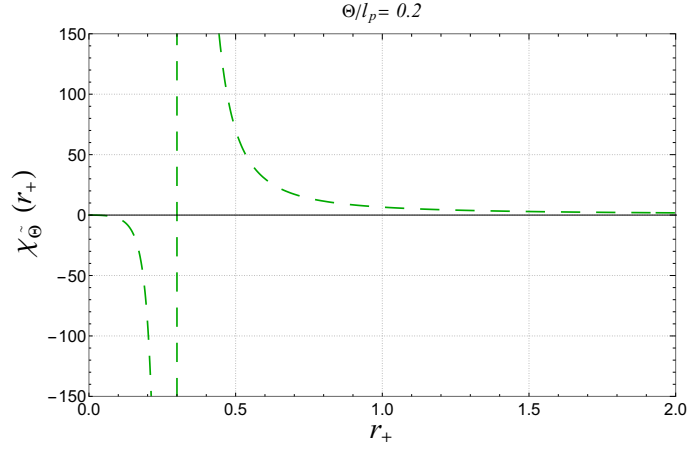


FIG. 9. Behavior of the NC susceptibility $\chi_{\tilde{\Theta}}$ as a function of the NC event horizon r_+ .

In Fig. III C we show the behavior of the susceptibility $\chi_{\tilde{\Theta}}$ as a function of the NC event horizon r_+ . The function $\chi_{\tilde{\Theta}}$ has a divergence at $r_+ = \frac{3}{2}\tilde{\Theta}$, which would indicate a continuous second-order critical point in the NC sector. However, this divergence is located inside the remnant region: the black hole stops radiating at $r_+ = 3\tilde{\Theta}$, so the singular point lies in a thermally inaccessible region for the semi-classical evaporation process. It is possible that a pure quantum evaporation process (forcing the black hole to complete evaporation, $m^{\min} \rightarrow 0$) could reach this region, in which case the divergence might be interpreted as a phase transition in the NC sector. As our model predicts a remnant at $r_+ = 3\tilde{\Theta}$, the only physically accessible region is the exterior of the remnant, $r_+ \geq 3\tilde{\Theta}$. In this region the NC susceptibility is positive, $\chi_{\tilde{\Theta}} > 0$, indicating a normal, stable linear response of the geometry to the deformation induced by non-commutativity. For large black holes the NC susceptibility is small, which indicates that the system becomes less sensitive to the NC parameter; this behavior is consistent with the mass (Fig. III A) and temperature (Fig. III A 1) profiles, where large changes in $\tilde{\Theta}$ induce only small changes in thermodynamic quantities. By contrast, for small black holes (regions closer to the remnant) the NC susceptibility is large, indicating that the system is highly sensitive to changes in $\tilde{\Theta}$: a small change in the NC parameter leads to large changes in the NC thermodynamic properties.

D. Thermodynamic properties of the NC charged black hole

In this subsection we compute several thermodynamic quantities to verify the consistency of the first law of black hole thermodynamics. We use the metric obtained above without a deformed mass Eq. (26) and work in the approximation regime.

a. *ADM mass:* We begin with the ADM mass, obtained by solving $f(r_+) = 0$,

$$m_Q = \frac{r_+^4 + Q^2 r_+^2 + 2aQ^3}{2r_+^3}, \quad (49)$$

which reduces to the RN mass in the commutative limit $\tilde{\Theta} = 0$. For $Q = 0$ the expression further reduces to the Schwarzschild mass.

b. *Temperature:* The NC-corrected black hole temperature is obtained from the surface gravity:

$$T_Q \simeq \frac{1}{4\pi r_+} - \frac{Q^2}{4\pi r_+^3} - \frac{3\tilde{\Theta}Q^3}{2\pi r_+^5}, \quad (50)$$

which reproduces the RN temperature when $\tilde{\Theta} = 0$, and the Schwarzschild temperature for $Q = 0$.

c. *Entropy:* We now use the first law of black hole thermodynamics (30) to derive the entropy. From $S_Q = \int dm/T$ and after expressing dm/T in terms of r one finds

$$S_Q = \int_0^{r_+} 2\pi r \frac{r^4 - Q^2(6\tilde{\Theta}Q + r^2)}{r^4 - Q^2 r^2 - 6\tilde{\Theta}Q^3} dr = 2\pi \int_0^{r_+} r dr,$$

$$= \pi r_+^2. \quad (51)$$

Thus the entropy equals the Bekenstein-Hawking area law, $S_Q = \pi r_+^2$. This result indicates that, in this setup, non-commutativity preserves the area law and the first law of black hole thermodynamics; this is because here the NC correction enters through the $U(1)$ interaction (gauge field) and not via a deformed mass contribution in the energy-momentum tensor as in the previous uncharged case.

IV. QUANTUM TUNNELING PROCESS

In this section we investigate quantum tunneling from the new NC black hole solution for both thermal and non-thermal radiation. To describe the tunneling process we employ regular (stationary) coordinates [30–32] that do not possess a coordinate singularity at the horizon, in contrast to the Schwarzschild-like coordinates; this choice guarantees conservation of energy during the derivation of the radiation spectrum. Concretely, we adopt the Painlevé-Gullstrand form [30–32, 41] to represent our NC black hole metric. For radial motion the line element (2) becomes

$$ds^2 = -f(r)cdt^2 + 2h(r)dtdr + dr^2 + r^2d\theta^2 + r^2\sin^2\theta d\phi^2, \quad (52)$$

where

$$h(r) = \sqrt{1 - f(r)}. \quad (53)$$

In the semi-classical tunneling picture the emission rate and the imaginary part of the action are related by [30–32]

$$\Gamma \sim e^{-2\text{Im}\hat{S}}. \quad (54)$$

Here \hat{S} denotes the NC tunneling action of the particle, defined for a particle moving freely in curved spacetime by

$$\hat{S} = \int p_\mu dx^\mu, \quad (55)$$

with conjugate momentum $p_\mu = \hat{g}_{\mu\nu} \frac{dx^\nu}{d\lambda}$ and affine parameter λ . We consider a massless particle on a radial trajectory in the equatorial plane $\theta = \pi/2$. The imaginary part of the action reduces to

$$\text{Im}\hat{S} = \text{Im} \int (p_t dt + p_r dr) = \text{Im} \int_{r_i}^{r_f} \int_0^{p_r} dp'_r dr. \quad (56)$$

The term involving p_t is real and therefore does not contribute to the imaginary part. Using Hamilton's equation $\dot{r} = \frac{dH}{dp_r}$ (where $\dot{r} = \frac{dr}{dt}$) and taking the system Hamiltonian as $H = m - \omega'^8$, Eq. (56) becomes

$$\text{Im}\hat{S} = \text{Im} \int_m^{m-\omega} \int_{r_i}^{r_f} \frac{d(m-\omega)}{\dot{r}} dr. \quad (57)$$

We assume that the tunneling particle follows the radial null geodesic (obtained from $\hat{g}_{\mu\nu}U^\mu U^\nu = 0$), whose radial velocity is

$$\frac{dr}{dt} = 1 - \sqrt{1 - f(r)}. \quad (58)$$

Expanding near the outer horizon r_+ gives

$$\frac{dr}{dt} \simeq \frac{1}{2}f'(r_+)(r - r_+) + \mathcal{O}((r - r_+)^2), \quad (59)$$

where the surface gravity is $\kappa(r_+) = \frac{1}{2}f'(r_+)$. Substituting this into Eq. (57) leads to

$$\text{Im}\hat{S} = \text{Im} \int_m^{m-\omega} \int \frac{d(m-\omega)}{\kappa(r_+)(r - r_+)} dr. \quad (60)$$

⁸ Where ω' represent the emitted particle energy.

A. Pure thermal radiation

In the pure thermal radiation case we have $\hat{g}_{01} = \hat{h}$ and $dH = d(m - \omega) = -d\omega$. After rearranging the expression in Eq. (60) we obtain

$$\text{Im } \hat{S} = \text{Im} \int_0^\omega (-d\omega) \int \frac{dr}{\kappa(r_+)(r - r_+)}. \quad (61)$$

The radial integral exhibits a simple pole at the event horizon $r = r_+$. We evaluate the integral using a contour deformation around the pole (residue theorem). Working in the low-frequency regime $\omega \ll m$ (so that the Boltzmann approximation $\Gamma \sim e^{-2\text{Im}\hat{S}} \sim e^{-\beta\omega}$ holds), and following the standard steps in Refs. [40, 83], we find

$$\text{Im } \hat{S} = \pi \int_0^\omega \frac{d\omega}{\kappa(r_+)} = \frac{\pi\omega}{\kappa(r_+)}. \quad (62)$$

1. Tunneling rate in thermal radiation

Substituting Eq. (62) into the tunneling-rate expression (54) yields

$$\Gamma \sim \exp \left[-4\pi\omega \frac{(\sqrt{m(m - 3\tilde{\Theta})} + m)^2}{\sqrt{m(m - 3\tilde{\Theta})} - 3\tilde{\Theta} + m} \right], \quad (63)$$

and in the leading order in the NC parameter one obtains

$$\Gamma \sim \exp \left[-2\pi\omega (4m + 3\tilde{\Theta}) \right]. \quad (64)$$

In the commutative limit $\tilde{\Theta} \rightarrow 0$ this reproduces the usual weak-energy result ($\omega \ll m$) [30, 32]. The above expression can be generalized to the charged NC black hole by using the corresponding surface gravity.

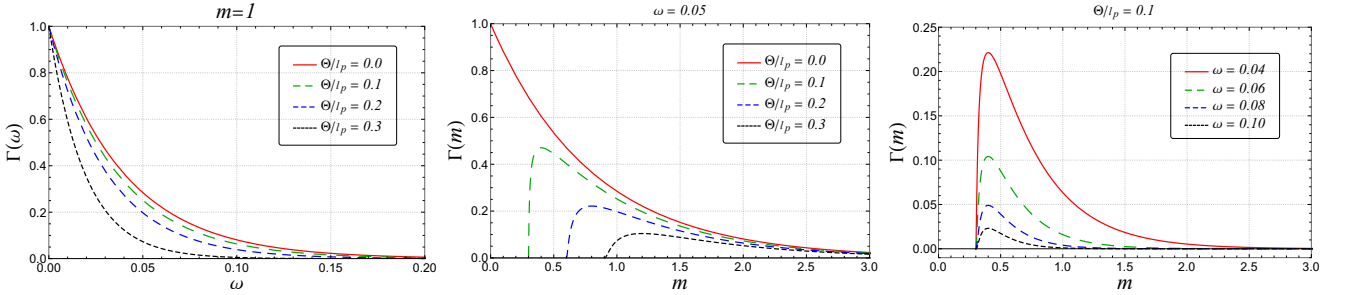


FIG. 10. Behavior of the tunneling rate Γ as a function of the NC outer event horizon r_+ and for different NC parameters $\tilde{\Theta}$.

Fig. 10 shows the tunneling rate Γ across the NC event horizon. The left panel displays Γ versus particle frequency ω and for different $\tilde{\Theta}$; the center panel shows Γ versus black hole mass m (for fixed ω), and the right panel shows Γ versus m for various ω . For the parameter ranges shown the NC correction reduces the tunneling rate, acting effectively as a barrier against particle escape. The qualitative behavior of the middle and right panels mirrors the temperature profile $T(r_+)$ (Fig. III A 1): during evaporation the tunneling rate increases to a maximum (corresponding to the maximum temperature) and then falls to zero when the black hole ceases to radiate.

a. *NC temperature* Assuming a purely thermal spectrum (Boltzmann factor), $\Gamma \sim e^{-\beta\omega}$ with $\beta = 1/T$, we obtain the compact temperature expression

$$T = \frac{\sqrt{m(m - 3\tilde{\Theta})} - 3\tilde{\Theta} + m}{4\pi(\sqrt{m(m - 3\tilde{\Theta})} + m)^2}, \quad (65)$$

which in the leading order reduces to the previously derived expression (32):

$$T = \frac{1}{8\pi m} - \frac{3\tilde{\Theta}}{32\pi m^2} = \frac{1}{4\pi r_+} - \frac{3\tilde{\Theta}}{4\pi r_+^2}. \quad (66)$$

2. Density number of particles

According to Refs. [41, 84–87], the particle-number density emitted can be computed from the tunneling rate. For our NC result (63) the emitted particle-number density is

$$n = \frac{\Gamma}{1 - \Gamma} = \frac{1}{e^{4\pi\omega \frac{(\sqrt{m(m-3\tilde{\Theta})+m})^2}{\sqrt{m(m-3\tilde{\Theta})-3\tilde{\Theta}+m}} - 1}}, \quad (67)$$

which, to leading order in the NC parameter, becomes

$$n = \frac{1}{e^{8\pi\omega \frac{4m^2}{4m-3\tilde{\Theta}} - 1}}. \quad (68)$$

It is worth noting that the above expression has the same form as the Planck distribution for black-body radiation and depends explicitly on the NC parameter that characterizes the deformed geometry. In the commutative limit $\tilde{\Theta} \rightarrow 0$, this particle-number density reduces to the standard expression [12]:

$$n = \frac{1}{e^{8\pi m\omega} - 1}. \quad (69)$$

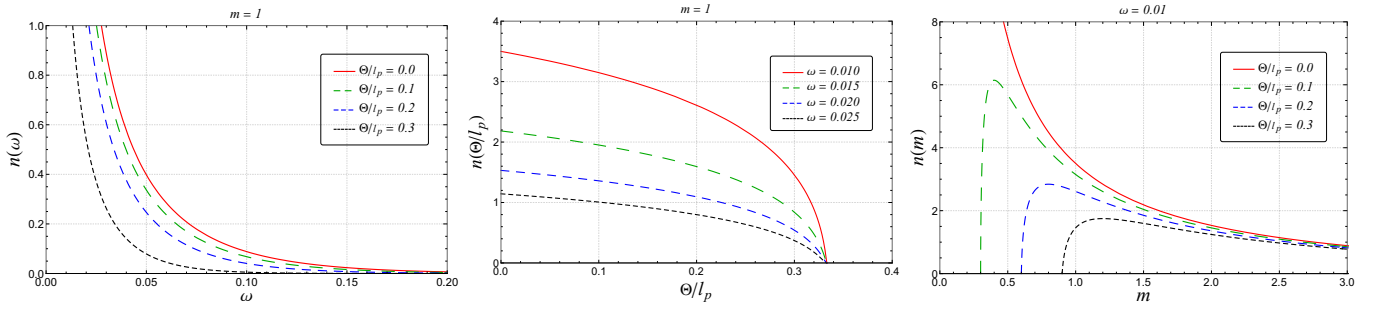


FIG. 11. Variation of the particle-number density n emitted from an NC black hole. Left: $n(\omega)$ for different $\tilde{\Theta}$ (fixed $m = 1$). Middle: $n(\tilde{\Theta})$ for different ω (fixed $m = 1$). Right: $n(m)$ for different $\tilde{\Theta}$ (fixed $\omega = 0.01$).

Fig. 11 shows the particle-number density n emitted by the NC Schwarzschild black hole as a function of the particle frequency ω (left panel). A key observation is the effect of non-commutativity: increasing the NC parameter $\tilde{\Theta}$ reduces the emitted particle-number density. This suppression resembles the effect of an effective potential barrier in quantum mechanics. The middle panel illustrates how non-commutativity lowers the emission density as $\tilde{\Theta}$ increases for several fixed frequencies. The right panel displays a behavior similar to the temperature profile $T(r_+)$ (see Fig. III A 1): as the black hole evaporates the emission density reaches a maximum (corresponding to the maximum temperature) and then decreases to zero when the black hole stops radiating. Thus non-commutativity effectively enhances the barrier against particle escape and explains the diminished emission density.

B. Non-thermal radiation

In this subsection we deal with the large-frequency regime ω and employ energy conservation. To proceed we use the definition (60) and integrate the relation (62) over the quantity $d(\hat{m} - \omega)$, which becomes

$$\text{Im}\hat{S} = \pi \int_m^{m-\omega} \frac{d(m-\omega)}{\kappa(m-\omega)} \quad (70)$$

According to Refs. [30, 32], the black hole mass in (62) is replaced by $m - \omega$. This substitution leads to the following expression:

$$\text{Im}\hat{S} = -\pi \int_m^{m-\omega} \left(\frac{(\sqrt{(m-\omega)((m-\omega)-3\tilde{\Theta}}) + (m-\omega))^2}{\sqrt{(m-\omega)((m-\omega)-3\tilde{\Theta}) - 3\tilde{\Theta} + (m-\omega)}} \right) d(m-\omega), \quad (71)$$

$$\begin{aligned}
&= -\pi \left((m-\omega)^2 + \frac{1}{2} \sqrt{(m-\omega)((m-\omega)-3\tilde{\Theta})} (9\tilde{\Theta} + 2(m-\omega)) - m^2 - \frac{1}{2} \sqrt{m(m-3\tilde{\Theta})} (9\tilde{\Theta} + 2m) \right. \\
&\quad \left. + \frac{27}{4} \tilde{\Theta}^2 \log \left(2 \left(\sqrt{(m-\omega)((m-\omega)-3\tilde{\Theta})} + (m-\omega) \right) - 3\tilde{\Theta} \right) - \frac{27}{4} \tilde{\Theta}^2 \log \left(2 \left(\sqrt{m(m-3\tilde{\Theta})} + m \right) - 3\tilde{\Theta} \right) \right),
\end{aligned} \tag{72}$$

The above equation represents the usual relation between the tunneling rate and entropy [30–32]:

$$\hat{\Gamma} \sim e^{-2Im\hat{S}} = e^{\Delta\hat{S}_{BH}}. \tag{73}$$

Here $\Delta\hat{S}_{BH} = \hat{S}_{BH}(m-\omega) - \hat{S}_{BH}(m)$. From this relation we obtain the following entropy expression:

$$\hat{S}_{BH} = 2\pi m^2 + \pi \sqrt{m(m-3\tilde{\Theta})} (9\tilde{\Theta} + 2m) \simeq \pi r_+^2 + 6\tilde{\Theta} r_+. \tag{74}$$

This entropy coincides with the expression obtained in Eq. (39); in the commutative limit we recover the Schwarzschild entropy. Up to second order we also observe the logarithmic correction mentioned above and found in gauge theory of gravity models [64, 65, 75].

1. Correlations

In what follows we investigate the effect of this NC approach on the statistical correlations between particles tunneling across the event horizon of the NC Schwarzschild black hole. To capture correlations we must expand the entropy to second order in the NC parameter, since there is no modification of the correlation at first order. Using Eq. (73) together with Eq. (71), the change of entropy is

$$\begin{aligned}
\Delta S &= -4\pi m\omega \left(1 - \frac{\omega}{2m} \right) + \frac{1}{2} \sqrt{(m-\omega)((m-\omega)-3\tilde{\Theta})} (9\tilde{\Theta} + 2(m-\omega)) - \frac{1}{2} \sqrt{m(m-3\tilde{\Theta})} (9\tilde{\Theta} + 2m) \\
&\quad + \frac{27}{2} \tilde{\Theta}^2 \log \left(\frac{2 \left(\sqrt{(m-\omega)((m-\omega)-3\tilde{\Theta})} + (m-\omega) \right) - 3\tilde{\Theta}}{2 \left(\sqrt{m(m-3\tilde{\Theta})} + m \right) - 3\tilde{\Theta}} \right),
\end{aligned} \tag{75}$$

and substituting this into Eq. (73) gives

$$\begin{aligned}
\hat{\Gamma} &= \left(\frac{2 \left(\sqrt{(m-\omega)((m-\omega)-3\tilde{\Theta})} + (m-\omega) \right) - 3\tilde{\Theta}}{2 \left(\sqrt{m(m-3\tilde{\Theta})} + m \right) - 3\tilde{\Theta}} \right)^{\frac{27\pi}{2} \tilde{\Theta}^2} \exp \left[-4\pi m\omega \left(1 - \frac{\omega}{2m} \right) + \frac{1}{2} \sqrt{(m-\omega)((m-\omega)-3\tilde{\Theta})} \right. \\
&\quad \left. \times (9\tilde{\Theta} + 2(m-\omega)) - \frac{1}{2} \sqrt{m(m-3\tilde{\Theta})} (9\tilde{\Theta} + 2m) \right].
\end{aligned} \tag{76}$$

Using the estimate $\tilde{\Theta} \sim l_{\text{Planck}}$ from Eq. (33) and expanding the entropy difference to second order in the NC parameter, the tunneling rate can be written as

$$\hat{\Gamma} = e^{\Delta\hat{S}_{BH}} = \left(\left(1 - \frac{\omega}{m} \right)^{\frac{27\pi}{2} l_{\text{Planck}}} e^{-6\pi\omega} \right)^{l_{\text{Planck}}} e^{-8\pi m\omega \left(1 - \frac{\omega}{2m} \right)}. \tag{77}$$

This expression contains an exponential factor reproducing the standard commutative non-thermal result [37] and a multiplicative correction that depends on the Planck length; the latter represents a quantum modification similar to that in Ref. [64]. The additional factor $e^{-6\pi\omega}$ originates from the first-order NC correction. In the semi-classical limit $l_{\text{Planck}} \rightarrow 0$ the correction vanishes and the commutative result is recovered [37].

We now investigate statistical correlations between successive emissions of energies ω_1 and ω_2 . Denote the single-emission rates by $\ln \Gamma_{\omega_1}$ and $\ln \Gamma_{\omega_2}$, and the combined emission by $\ln \Gamma_{\omega_1+\omega_2}$. Following Refs. [88–90], the statistical correlation is

$$\chi(\omega_1 + \omega_2; \omega_1, \omega_2) = \ln \left(\frac{\ln \hat{\Gamma}_{\omega_1+\omega_2}}{\ln \hat{\Gamma}_{\omega_1} + \ln \hat{\Gamma}_{\omega_2}} \right)$$

$$\begin{aligned}
&= 4\pi\omega_1\omega_2 + \pi\sqrt{m(m-3\tilde{\Theta})}(9\tilde{\Theta}+2m) - \pi\sum_{i=1}^2\sqrt{(m-\omega_i)(-3a+m-\omega_i)}(9\tilde{\Theta}+2m-2\omega_i) \\
&+ \pi\sqrt{(m-\omega_1-\omega_2)(-3a+m-(\omega_1+\omega_2))}(9\tilde{\Theta}+2m-2(\omega_1+\omega_2)) \\
&+ \frac{27}{2}\pi\tilde{\Theta}^2\ln\left[\frac{A(m)A(m-(\omega_1+\omega_2))}{A(m-\omega_1)A(m-\omega_2)}\right], \tag{78}
\end{aligned}$$

where

$$A(m) = 2\left(\sqrt{m(m-3a)} + m\right) - 3a. \tag{79}$$

The statistical correlation function remains nonzero in this NC gauge theory approach, as in the commutative case [39, 88–90]. Thus different radiation frequencies during black hole evaporation remain correlated ($\chi \neq 0$). Non-commutativity reduces the statistical correlations between successive emissions: the modified geometry acts like an effective potential well that suppresses particle tunneling across the horizon and weakens their mutual correlations. The existence of correlations among emitted quanta indicates that information can be carried by Hawking radiation, which addresses the information-loss problem. In this NC framework information is preserved in a remnant (see Sec. III A 1); the geometric suppression of correlations is consistent with mechanisms by which information may escape the horizon, akin to “hidden messengers in Hawking radiation” [88].

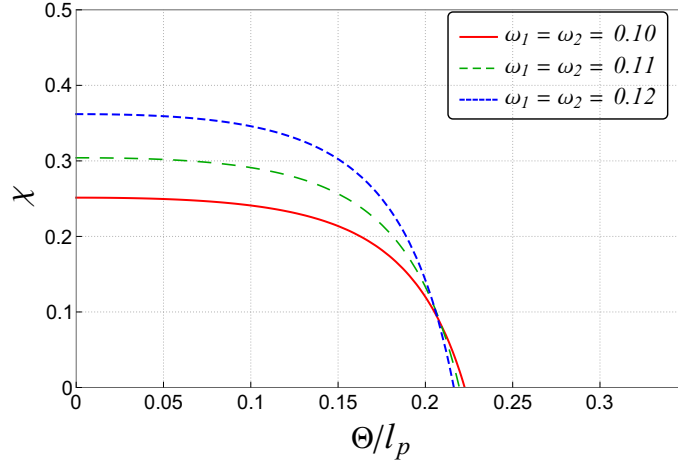


FIG. 12. Variation of the statistical correlation function χ as a function of the NC parameter $\tilde{\Theta}$ for different frequencies ω_i .

Fig. 12 shows the behavior of the statistical correlation function χ as a function of the NC parameter $\tilde{\Theta}$ for different particle frequencies ω . Non-commutativity reduces the correlation between two successive emitted particles, while increasing the particle energies strengthens the correlation: higher-energy emissions carry more information, whereas lower-energy emissions carry less. Moreover, the leading-order expression of the correlation reads

$$\chi(\omega_1 + \omega_2; \omega_1, \omega_2) \simeq 8\pi\omega_1\omega_2 + \frac{27\pi}{2}\tilde{\Theta}^2\ln\left(\frac{m(m-(\omega_1+\omega_2))}{(m-\omega_1)(m-\omega_2)}\right), \tag{80}$$

which matches the result obtained in NC gauge theory of gravity studies [64, 65]. In the limit $\tilde{\Theta} = 0$ we recover the commutative correlation function [39, 88–90].

V. CONCLUSION

In this work, we have presented a novel approach to constructing black hole solutions within the framework of NC gauge theory by applying the Seiberg-Witten (SW) map to the interaction potential and subsequently solving Einstein’s field equations for the resulting deformed gauge potential. We analyzed the geometric properties of both NC Schwarzschild and Reissner-Nordström (RN) black holes, presenting the metrics in both compact forms and as expansions in terms of the NC

parameter Θ . Our results demonstrate that the NC metric exhibits similarities with certain regular black hole solutions and NC matter distributions in its compact form. In the approximate limit, the curvature function behaves similarly to the RN black hole solution characterized by two horizons (inner and outer). Furthermore, this geometry leads to a reduction of the event horizon radius, such that $r_+ < 2m$.

Subsequently, we investigated the thermodynamic properties of the NC Schwarzschild black hole and the influence of this geometry on thermal stability. We computed the ADM mass, Hawking temperature, and entropy for both NC Schwarzschild and RN black holes. Our findings indicate that non-commutativity predicts a new minimum in the final stage of evaporation for the ADM mass profile, consistent with other NC geometric models [62]. This framework effectively removes the temperature divergence, leading to a cold remnant as the black hole ceases radiation. Moreover, the entropy displays a second-order logarithmic correction, deviating from the area law due to the inclusion of the NC geometry as a modified matter distribution via the energy-momentum tensor. However, when extending this to the NC RN case without mass-term corrections, the area law and the first law of black hole thermodynamics remain valid (see SubSec. III D). Estimation of the NC parameter from the temperature profile yields a bound located at the Planck scale, $\Theta \sim l_p$, aligning with NC gauge gravity models [62, 64, 75]. This approach facilitates the study of black hole physics in a manner analogous to the commutative RN case.

Furthermore, we examined the heat capacity of the NC Schwarzschild black hole, identifying a divergence at a critical point r_+^{crit} , which corresponds to the state of maximal radiation (maximum temperature T^{max}). At this point, a second-order phase transition occurs from an unstable large black hole to a stable small black hole, a behavior absent in commutative solutions. Thermal stability was further verified through the Helmholtz free energy, which exhibits two extrema: a maximum representing the unstable large black hole and a minimum representing the stable small black hole, consistent with the heat capacity profile in Fig. III A 3. These results indicate that larger black holes are thermally unstable, while smaller ones are stable, eventually resulting in a cooled remnant. Upon introducing pressure, we observed three distinct regimes around the critical pressure P_C : for $P < P_C$, a quasi-swallowtail structure emerges with smooth curves; at $P = P_C$, an inflection point appears, corresponding to a Hawking-Page-like phase transition [62, 65], and this point disappears for $P > P_C$. This signifies a second-order phase transition consistent with standard thermodynamic theories. Moreover, we have investigated the susceptibility and linear response of this black hole to changes in the Θ , where we find that, the small black hole show high sensitivity to small changes in Θ , while for larger ones the sensitivity becomes weaker, which is in good accordance with the profiles of black hole mass and temperature profiles.

Finally, we investigated the effect of non-commutativity on quantum tunneling from the event horizon. We employed a semi-classical tunneling approach across two scenarios. First, we examined pure thermal radiation characterized by the emission of massless particles at low frequencies. This process reproduced the thermal properties obtained via the geometric approach, confirming that non-commutativity preserves this equivalence [64]. We found that the geometry reduces the tunneling rate, akin to a potential well in quantum mechanics, and leads to a zero tunneling rate in the final stages of evaporation, further confirming the existence of a cold remnant (see Fig. III A 1). A similar effect was observed for the particle number density, where the geometry enhances the barrier against tunneling. In the second scenario, we examined non-thermal radiation by considering energy conservation [32], particularly for high-frequency emissions. We found that the non-thermal tunneling rate is consistent with a unitary quantum theory, related to the entropy difference. This entropy exhibits a second-order logarithmic correction in the NC parameter with a coefficient tied to the Planck length l_p , representing a quantum surface at the Planck scale. These results align with other quantum gravity candidates, including Loop Quantum Gravity (LQG), String Theory, the Generalized Uncertainty Principle (GUP), and Modified Dispersion Relations (MDR) [3, 6, 7, 52, 91], and in particular similar to the one obtained from thermal fluctuations correction [92–94]. Finally, we analyzed the statistical correlation between two successively emitted particles with energies ω_1 and ω_2 . Our results show that non-commutativity reduces this correlation: as the NC parameter Θ increases, the correlation weakens, reaching zero under specific conditions on Θ and the frequencies, and eventually becoming negative ($\chi < 0$) for high Θ values.

Appendix A: Non-commutative correction to the Schwarzschild-De-Sitter black hole

In this appendix we present the NC correction to Schwarzschild-De-Sitter black hole, where the commutative solution is given by:

$$f(r) = 1 - \frac{2m}{r} - \frac{\Lambda}{3}r^2, \quad (\text{A1})$$

The Einstein equation in this case become:

$$G_\nu^\mu - \Lambda\delta_\nu^\mu = T_\nu^\mu \quad (\text{A2})$$

As the cosmological term is constant term, so there is no gauge correction, for that we use the NC matter correction given by Eq. (12) resulting from the NC Newton gauge potential $\hat{\Phi}_N$. For that, the final NC curvature function written as follow:

$$\begin{aligned} f_\Lambda(r) &= 1 - \frac{2mr}{(r^2 + 3m\tilde{\Theta})} - \frac{\Lambda}{3}r^2 \\ &\simeq 1 - \frac{2m}{r} + \frac{6m^2}{r^3}\tilde{\Theta} - \frac{\Lambda}{3}r^2, \end{aligned} \quad (\text{A3})$$

It is clear that, in the commutative limit $\alpha = 0$ we recover the Schwarzschild-De-Sitter black hole [71].

If one want to compute the NC correction to the cosmological term, its necessary to introducing the cosmological term in Newton potential and not from Einstein equation [95]:

$$\Phi_{N,\Lambda} = -\frac{GM}{r} - \frac{\Lambda c^2 r^2}{6}, \quad (\text{A4})$$

By following the same procedure in Sec. II, we find the NC gauge potential for Newton plus cosmological term:

$$\hat{\Phi}_N = -\frac{GM}{r} - \frac{\Lambda c^2 r^2}{6} + \frac{\Theta}{l_p c^2} \left(\frac{G^2 M^2}{r^3} + \frac{\Lambda c^2 GM}{2} - \frac{\Lambda^2 c^4 r^3}{18} \right), \quad (\text{A5})$$

The NC total density for the region $r > 0$, become:

$$\hat{\rho}_N + \hat{\rho}_\Lambda = \tilde{\Theta} \frac{3GM^2}{2\pi c^2 r^5} + \frac{\Lambda c^2}{8\pi G} - \tilde{\Theta} \frac{\Lambda^2 c^2 r}{6\pi G}, \quad (\text{A6})$$

As we see there is no correction to the first order of the cosmological constant. Then we find the NC curvature function for Schwarzschild-De-Sitter black hole:

$$\begin{aligned} f_\Lambda(r) &= 1 - \frac{2mr}{(r^2 + 3m\tilde{\Theta})} - \frac{\Lambda r^2}{3(1 + \Lambda\tilde{\Theta})}, \\ &\simeq 1 - \frac{2m}{r} + \frac{6m^2}{r^3}\tilde{\Theta} - \frac{\Lambda}{3}r^2 + \frac{\Lambda^2 r^3 \tilde{\Theta}}{3}, \end{aligned} \quad (\text{A7})$$

As we know the cosmological constant so small parameter $\Lambda \propto 10^{-51} m^{-2}$, and multiplied by NC parameter which is expected to be in order of Planck length, so the second order correction to the cosmological constant can be negligible compared to the others terms for small distance and we recover solution (A3). While for very large distance $r \rightarrow \infty$, this term may be the dominant one.

Appendix B: Non-commutative correction to the Reissner-Nordström-De-Sitter black hole

The NC metric of the Reissner-Nordström-De-Sitter black hole, can be derived as the above one. For that, we have two different scenarios, where the first one we compute the NC correction only to the Coulomb gauge potential where we use NC Maxwell energy-momentum tensor (23), and that give us the following NC RN-dS black hole solution:

$$\begin{aligned} f_{Q,\Lambda}(r) &= 1 - \frac{2m}{r} + \frac{Q^2}{(r^2 - 2\tilde{\Theta}Q)} - \frac{\Lambda}{3}r^2, \\ &\simeq 1 - \frac{2m}{r} + \frac{Q^2}{r^2} + \frac{2\tilde{\Theta}Q^3}{r^4} - \frac{\Lambda}{3}r^2. \end{aligned} \quad (\text{B1})$$

Where in the limit of $\tilde{\Theta} \rightarrow 0$, we recover the commutative solution [96]. The second scenario is the include of the NC matter correction including the cosmological constant in Newton potential that given by expressions (11) and (A6) together with (23). For that we get:

$$\begin{aligned} f_{Q,\Lambda}(r) &= 1 - \frac{mr}{(r^2 + 3m\tilde{\Theta})} + \frac{Q^2}{(r^2 - 2\tilde{\Theta}Q)} - \frac{\Lambda r^2}{3(1 + \Lambda\tilde{\Theta})}, \\ &\simeq 1 - \frac{2m}{r} + \frac{Q^2}{r^2} + \left(\frac{6m^2}{r^3} + \frac{2Q^3}{r^4} \right) \tilde{\Theta} - \frac{\Lambda}{3}r^2 + \frac{\Lambda^2 r^3 \tilde{\Theta}}{3}. \end{aligned} \quad (\text{B2})$$

and for small distance, the second order in cosmological constant become negligible, and that yield to the following metric:

$$f_{Q,\Lambda}(r) \simeq 1 - \frac{2m}{r} + \frac{Q^2}{r^2} + \left(\frac{6m^2}{r^3} + \frac{2Q^3}{r^4} \right) \tilde{\Theta} - \frac{\Lambda}{3}r^2. \quad (\text{B3})$$

ACKNOWLEDGMENTS

-
- [1] Dieter Lüst and Stefan Theisen, *Lectures on string theory*, Vol. 346 (Springer, 1989).
- [2] Ralph Blumenhagen, Dieter Lüst, and Stefan Theisen, *Basic concepts of string theory*, Vol. 17 (Springer, 2013).
- [3] Sergey N Solodukhin, "Entropy of the schwarzschild black hole and the string–black-hole correspondence," *Physical Review D* **57**, 2410 (1998).
- [4] Carlo Rovelli, *Quantum gravity* (Cambridge university press, 2004).
- [5] Carlo Rovelli, "Loop quantum gravity," *Living reviews in relativity* **11**, 1–69 (2008).
- [6] Krzysztof A Meissner, "Black-hole entropy in loop quantum gravity," *Classical and Quantum Gravity* **21**, 5245 (2004).
- [7] Amit Ghosh and Parthasarathi Mitra, "Log correction to the black hole area law," *Physical Review D* **71**, 027502 (2005).
- [8] Daniel Z Freedman and P Van Nieuwenhuizen, "Properties of supergravity theory," *Physical Review D* **14**, 912 (1976).
- [9] Stanley D Deser and Bruno Zumino, "Consistent supergravity," *Phys. Lett. B* **62**, 335–337 (1976).
- [10] Daniel Z Freedman, P van Nieuwenhuizen, and Sergio Ferrara, "Progress toward a theory of supergravity," in *Supergravities in Diverse Dimensions: Commentary and Reprints (In 2 Volumes)* (World Scientific, 1989) pp. 512–516.
- [11] P. van Nieuwenhuizen, "Supergravity," *Physics Reports* **68**, 189–398 (1981).
- [12] Stephen W Hawking, "Particle creation by black holes," in *Euclidean quantum gravity* (World Scientific, 1975) pp. 167–188.
- [13] G. W. Gibbons and S. W. Hawking, "Cosmological event horizons, thermodynamics, and particle creation," *Phys. Rev. D* **15**, 2738–2751 (1977).
- [14] James M Bardeen, Brandon Carter, and Stephen W Hawking, "The four laws of black hole mechanics," *Communications in mathematical physics* **31**, 161–170 (1973).
- [15] B Harms and Y Leblanc, "Statistical mechanics of black holes," *Physical Review D* **46**, 2334 (1992).
- [16] Cenalo Vaz, "Canonical quantization and the statistical entropy of the schwarzschild black hole," *Physical Review D* **61**, 064017 (2000).
- [17] Ioannis Haranas and Ioannis Gkigkitzis, "Entropic gravity resulting from a yukawa type of correction to the metric for a solar mass black hole," *Astrophysics and Space Science* **347**, 77–82 (2013).
- [18] Devin Hansen, David Kubizňák, and Robert B Mann, "Criticality and surface tension in rotating horizon thermodynamics," *Classical and Quantum Gravity* **33**, 165005 (2016).
- [19] Abdul Jawad and Amna Khawer, "Thermodynamic consequences of well-known regular black holes under modified first law," *The European Physical Journal C* **78**, 1–10 (2018).
- [20] Deyou Chen, Jun Tao, *et al.*, "The modified first laws of thermodynamics of anti-de sitter and de sitter space–times," *Nuclear Physics B* **918**, 115–128 (2017).
- [21] James W York Jr, "Black-hole thermodynamics and the euclidean einstein action," *Physical Review D* **33**, 2092 (1986).
- [22] MM Akbar and Saurya Das, "Entropy corrections for schwarzschild and reissner–nordström black holes," *Classical and Quantum Gravity* **21**, 1383 (2004).
- [23] Andrew P Lundgren, "Charged black hole in a canonical ensemble," *Physical Review D* **77**, 044014 (2008).
- [24] Shahjalal Md, "Phase transition of quantum-corrected schwarzschild black hole in rainbow gravity," *Physics Letters B* **784**, 6–11 (2018).
- [25] Peng Wang, Houwen Wu, and Haitang Yang, "Thermodynamics and phase transition of a nonlinear electrodynamic black hole in a cavity," *Journal of High Energy Physics* **2019**, 1–19 (2019).
- [26] Peng Wang, Houwen Wu, Haitang Yang, and Feiyu Yao, "Extended phase space thermodynamics for black holes in a cavity," *Journal of High Energy Physics* **2020**, 1–19 (2020).
- [27] Steven M Christensen and Stephen A Fulling, "Trace anomalies and the hawking effect," *Physical Review D* **15**, 2088 (1977).
- [28] Sean P Robinson and Frank Wilczek, "Relationship between hawking radiation and gravitational anomalies," *Physical review letters* **95**, 011303 (2005).
- [29] Rabin Banerjee and Shailesh Kulkarni, "Hawking radiation and covariant anomalies," *Physical Review D* **77**, 024018 (2008).
- [30] Maulik K Parikh and Frank Wilczek, "Hawking radiation as tunneling," *Physical review letters* **85**, 5042 (2000).
- [31] Maulik Parikh, "A secret tunnel through the horizon," *General Relativity and Gravitation* **36**, 2419–2422 (2004).
- [32] Maulik K Parikh, "Energy conservation and hawking radiation," *arXiv preprint hep-th/0402166* (2004).
- [33] K Srinivasan and T Padmanabhan, "Particle production and complex path analysis," *Physical Review D* **60**, 024007 (1999).
- [34] Samuli Hemming and Esko Keski-Vakkuri, "Hawking radiation from ads black holes," *Physical Review D* **64**, 044006 (2001).
- [35] Elias C Vagenas, "Semiclassical corrections to the bekenstein–hawking entropy of the btz black hole via self-gravitation," *Physics Letters B* **533**, 302–306 (2002).
- [36] Jingyi Zhang and Zheng Zhao, "Hawking radiation via tunneling from kerr black holes," *Modern Physics Letters A* **20**, 1673–1681 (2005).
- [37] Michele Arzano, A Joseph M Medved, and Elias C Vagenas, "Hawking radiation as tunneling through the quantum horizon," *Journal of High Energy Physics* **2005**, 037 (2005).
- [38] P Mitra, "Hawking temperature from tunnelling formalism," *Physics Letters B* **648**, 240–242 (2007).
- [39] L Vanzo, G Acquaviva, and R Di Criscienzo, "Tunnelling methods and hawking's radiation: achievements and prospects," *Classical and Quantum Gravity* **28**, 183001 (2011).

- [40] Yang Liu, "The effect of quantum correction on hawking radiation for schwarzschild black holes," arXiv preprint arXiv:2201.00599 (2022).
- [41] Xavier Calmet, Stephen DH Hsu, and Marco Sebastianutti, "Quantum gravitational corrections to particle creation by black holes," *Physics Letters B*, 137820 (2023).
- [42] Zhong-Wen Feng and Shu-Zheng Yang, "Thermodynamic phase transition of a black hole in rainbow gravity," *Physics Letters B* **772**, 737–742 (2017).
- [43] Zhong-Wen Feng, Xia Zhou, Shi-Qi Zhou, and Dan-Dan Feng, "Rainbow gravity corrections to the information flux of a black hole and the sparsity of hawking radiation," *Annals of Physics* **416**, 168144 (2020).
- [44] Zi-Yu Fu and Hui-Ling Li, "The effect of gup on thermodynamic phase transition of rutz-schwarzschild black hole," *Nuclear Physics B* **969**, 115475 (2021).
- [45] Bilel Hamil and BC Lütüoğlu, "Effect of the modified heisenberg algebra on the black hole thermodynamics," *Europhysics Letters* **133**, 30003 (2021).
- [46] B Hamil and BC Lütüoğlu, "The effect of higher-order extended uncertainty principle on the black hole thermodynamics," *Europhysics Letters* **134**, 50007 (2021).
- [47] B Hamil, BC Lütüoğlu, and L Dahbi, "Eup-corrected thermodynamics of btz black hole," *International Journal of Modern Physics A* **37**, 2250130 (2022).
- [48] Yen Chin Ong, "An effective black hole remnant via infinite evaporation time due to generalized uncertainty principle," *Journal of High Energy Physics* **2018**, 1–11 (2018).
- [49] Luciano Petruzzello, "Generalized uncertainty principle with maximal observable momentum and no minimal length indeterminacy," *Classical and Quantum Gravity* **38**, 135005 (2021).
- [50] Khireddine Nouicer, "Quantum-corrected black hole thermodynamics to all orders in the planck length," *Physics Letters B* **646**, 63–71 (2007).
- [51] Kourosh Nozari and AS Sefidgar, "On the existence of the logarithmic correction term in black hole entropy-area relation," *General Relativity and Gravitation* **39**, 501–509 (2007).
- [52] Kourosh Nozari and AS Sefidgar, "Comparison of approaches to quantum correction of black hole thermodynamics," *Physics Letters B* **635**, 156–160 (2006).
- [53] Alain Connes, *Noncommutative geometry* (Springer, 1994).
- [54] Nathan Seiberg and Edward Witten, "String theory and noncommutative geometry," *Journal of High Energy Physics* **1999**, 032 (1999).
- [55] Robert H Brandenberger, "String theory, space-time non-commutativity and structure formation," *Progress of Theoretical Physics Supplement* **171**, 121–132 (2007).
- [56] AA Araújo Filho, JR Nascimento, A Yu Petrov, PJ Porfírio, and Ali Övgün, "Effects of non-commutative geometry on black hole properties," *Physics of the Dark Universe* **46**, 101630 (2024).
- [57] Kourosh Nozari and S Hamid Mehdipour, "Hawking radiation as quantum tunneling from a noncommutative schwarzschild black hole," *Classical and Quantum Gravity* **25**, 175015 (2008).
- [58] Piero Nicolini, Anais Smalagic, and Euro Spallucci, "Noncommutative geometry inspired schwarzschild black hole," *Physics Letters B* **632**, 547–551 (2006).
- [59] Sushant G Ghosh, "Noncommutative geometry inspired einstein–gauss–bonnet black holes," *Classical and Quantum Gravity* **35**, 085008 (2018).
- [60] Kourosh Nozari and Behnaz Fazlpour, "Reissner-nordström black hole thermodynamics in noncommutative spaces," (2006), [arXiv:gr-qc/0608077 \[gr-qc\]](https://arxiv.org/abs/gr-qc/0608077).
- [61] KOUROSH NOZARI and BEHNAZ FAZLPOUR, "Thermodynamics of noncommutative schwarzschild black hole," *Modern Physics Letters A* **22**, 2917–2930 (2007), <https://doi.org/10.1142/S0217732307023602>.
- [62] Abdellah Touati and Slimane Zaim, "Thermodynamic properties of schwarzschild black hole in non-commutative gauge theory of gravity," *Annals of Physics* **455**, 169394 (2023).
- [63] A.A. Araújo Filho, S. Zare, P.J. Porfírio, J. Kříž, and H. Hassanabadi, "Thermodynamics and evaporation of a modified schwarzschild black hole in a non-commutative gauge theory," *Physics Letters B* **838**, 137744 (2023).
- [64] Abdellah Touati and Zaim Slimane, "Quantum tunneling from schwarzschild black hole in non-commutative gauge theory of gravity," *Physics Letters B* **848**, 138335 (2024).
- [65] Abdellah Touati, "Non-commutative gauge theory and quantum gravity," Ph. D. Thesis (2024).
- [66] Ali H Chamseddine, "Deforming einstein's gravity," *Physics Letters B* **504**, 33–37 (2001).
- [67] Tajron Jurić, A Naveena Kumara, and Filip Požar, "Constructing noncommutative black holes," *Nuclear Physics B*, 116950 (2025).
- [68] Kourosh Nozari and Sara Islamzadeh, "Tunneling of massive and charged particles from noncommutative reissner-nordström black hole," *Astrophysics and Space Science* **347**, 299–304 (2013).
- [69] Sean M Carroll, *Spacetime and geometry* (Cambridge University Press, 2019).
- [70] Abdellah Touati and Slimane Zaim, "Lyapunov exponents and geodesic stability of schwarzschild black hole in the non-commutative gauge theory of gravity," *Nuclear Physics B*, 117018 (2025).
- [71] Chandrasekhar Subrahmanyan, *Mathematical Theory of Black Holes* (Oxford University Press, 1999).
- [72] Muhammad Sharif and Ghulam Abbas, "Non-commutative correction to thin shell collapse in reissner–nordström geometry," *Journal of the Physical Society of Japan* **81**, 044002 (2012).
- [73] Saeed Noori Gashti, Yassine Sekhmani, Mohammad Ali S Afshar, Mohammad Reza Alipour, Mohammadreza Khodajou Masouleh, Behnam Pourhassan, Jafar Sadeghi, and Javlon Rayimbaev, "Thermodynamic signatures in black hole geometry and harmonic

- oscillations with nonlinear electromagnetic fields and phantom global monopole," *Nuclear Physics B* , 117244 (2025).
- [74] Wontae Kim, Edwin J Son, and Myungseok Yoon, "Thermodynamic similarity between the noncommutative schwarzschild black hole and the reissner-nordström black hole," *Journal of High Energy Physics* **2008**, 042 (2008).
- [75] Abdellah Touati and Slimane Zaim, "Schwarzschild black hole surrounded by a cavity and phase transition in the non-commutative gauge theory of gravity," *Astroparticle Physics* **161**, 102988 (2024).
- [76] Slimane Zaim and Hadjar Rezki, "Thermodynamic properties of a yukawa-schwarzschild black hole in noncommutative gauge gravity," *Gravitation and Cosmology* **26**, 200–207 (2020).
- [77] Rui-Bo Wang, Shi-Jie Ma, Lei You, Jian-Bo Deng, and Xian-Ru Hu, "Thermodynamics of schwarzschild-ads black hole in non-commutative geometry," *Chinese Physics C* **49**, 065101 (2025).
- [78] Kourosh Nozari and S Hamid Mehdipour, "Hawking radiation as quantum tunneling from a noncommutative schwarzschild black hole," *Classical and Quantum Gravity* **25**, 175015 (2008).
- [79] Rong-Gen Cai, "Gauss-bonnet black holes in ads spaces," *Physical Review D* **65**, 084014 (2002).
- [80] Sharmila Gunasekaran, David Kubizňák, and Robert B Mann, "Extended phase space thermodynamics for charged and rotating black holes and born-infeld vacuum polarization," *Journal of High Energy Physics* **2012**, 1–43 (2012).
- [81] Julio A Méndez-Zavaleta, Efraín Rojas, and José Joaquín Suárez-Garibay, "Classical emergence of the quantum-backreacted btz black hole from exponential electrodynamics," *arXiv preprint arXiv:2601.18967* (2026).
- [82] Anurag Sahay, Tapobrata Sarkar, and Gautam Sengupta, "On the phase structure and thermodynamic geometry of r-charged black holes," *Journal of High Energy Physics* **2010**, 1–33 (2010).
- [83] George Johnson and John March-Russell, "Hawking radiation of extended objects," *Journal of High Energy Physics* **2020**, 1–16 (2020).
- [84] Sigurd Sannan, "Heuristic derivation of the probability distributions of particles emitted by a black hole," *General Relativity and Gravitation* **20**, 239–246 (1988).
- [85] HS Vieira, VB Bezerra, and GV Silva, "Analytic solutions in the dyon black hole with a cosmic string: scalar fields, hawking radiation and energy flux," *Annals of Physics* **362**, 576–592 (2015).
- [86] HS Vieira and VB Bezerra, "Confluent heun functions and the physics of black holes: resonant frequencies, hawking radiation and scattering of scalar waves," *Annals of Physics* **373**, 28–42 (2016).
- [87] George Johnson, "Tunnelling of charged particles from black holes," *Journal of High Energy Physics* **2020** (2020), [10.1007/jhep03\(2020\)038](https://doi.org/10.1007/jhep03(2020)038).
- [88] Baocheng Zhang, Qing-yu Cai, Li You, and Ming-sheng Zhan, "Hidden messenger revealed in hawking radiation: a resolution to the paradox of black hole information loss," *Physics Letters B* **675**, 98–101 (2009).
- [89] Baocheng Zhang, Qing-yu Cai, Ming-sheng Zhan, and Li You, "Entropy is conserved in hawking radiation as tunneling: a revisit of the black hole information loss paradox," *Annals of Physics* **326**, 350–363 (2011).
- [90] Baocheng Zhang, Qing-yu Cai, Ming-sheng Zhan, and Li You, "Information conservation is fundamental: Recovering the lost information in hawking radiation," *International Journal of Modern Physics D* **22**, 1341014 (2013).
- [91] Kourosh Nozari and AS Sefidgar, "On the existence of the logarithmic correction term in black hole entropy-area relation," *General Relativity and Gravitation* **39**, 501–509 (2007).
- [92] G Abbas and RH Ali, "Thermal fluctuations, quasi-normal modes and phase transition of the charged ads black hole with perfect fluid dark matter," *The European Physical Journal C* **83**, 407 (2023).
- [93] Zunaira Akhtar, Rimsha Babar, and Riasat Ali, "Thermal fluctuations evolution of the new schwarzschild black hole," *Annals of Physics* **448**, 169190 (2023).
- [94] Shahid Chaudhary, Atiq ur Rehman, Mohsan Ali, and Ahmad A Ifseisi, "Effects of thermal fluctuations on the evaporation of ads schwarzschild scalar tensor vector gravity black hole," *Journal of High Energy Astrophysics* **43**, 31–43 (2024).
- [95] Michael Paul Hobson, George P Efstathiou, and Anthony N Lasenby, *General relativity: an introduction for physicists* (Cambridge university press, 2006).
- [96] Ran Li, Kun Zhang, and Jin Wang, "Thermal dynamic phase transition of reissner-nordström anti-de sitter black holes on free energy landscape," *Journal of High Energy Physics* **2020**, 1–25 (2020).